



Addis Ababa University
Addis Ababa Institute of Technology
Department of Electrical and Computer Engineering

**DESIGN OF A PHOTOVOLTAIC-WIND HYBRID POWER
GENERATION SYSTEM FOR ETHIOPIAN REMOTE AREA**

A thesis Submitted to the Addis Ababa Institute of Technology, School of
Graduate Studies, Addis Ababa University
In partial fulfillment of the Requirement for the Degree of MASTERS OF
SCIENCE IN ELECTRICAL ENGINEERING (ELECTRICAL POWER
ENGINEERING)

By Gelma Boneya

Advisor Dr. Getachew Bekele

July 2011

Addis Ababa, Ethiopia



Addis Ababa University
Addis Ababa Institute of Technology
Department of Electrical and Computer Engineering

**DESIGN OF A PHOTOVOLTAIC-WIND HYBRID POWER
GENERATION SYSTEM FOR ETHIOPIAN REMOTE AREA**

By Gelma Boneya Huka

APPROVED BY BOARD OF EXAMINERS

Dr.-Ing. Getahun Mekuria

Chairman, Department of Electrical
and Computer Engineering

Signature

Dr. Getachew Bekele

Advisor

Signature

Dr. Frehiwot W/Hanna

Internal Examiner

Signature

Prof. W/Ghiorgis W/Mariam

External Examiner

Signature

DECLARATION

I, the undersigned, declare that this thesis is my original work, has not been presented for a degree in this or other universities, all sources of materials used for this thesis work have been fully acknowledged.

Name: Gelma Boneya Signature: _____

Place: Addis Ababa Institute of Technology, Addis Ababa University, Addis Ababa

Date of Submission: _____

This thesis has been submitted for examination with my approval as a university advisor.

Dr. Getachew Bekele Signature _____

Advisor's Name

*Dedicated to my parents Boneya and Dhaki,
brothers & sisters and all who live
without electricity*

ACKNOWLEDGEMENT

First and foremost, I take this opportunity to give glory to the almighty God without which the completion of this work would have been impossible.

Next, I would like to express my sincere gratitude to my advisors Dr. Getachew Bekele for his expert guidance, constructive comments, suggestions and encouragement without which this work could have not been completed. He has been a constant source of inspiration throughout lifespan of my study.

I owe my greatest gratitude to my parents especially to my beloved mother, who has been the inspiration of my life; your passion for education has contributed immensely to the completion of this study, this is for you.

Lastly but certainly not the least important, I would like to thank all the people stood by my side.

Addis Ababa, July 2011

TABLE OF CONTENTS

ACKNOWLEDGEMENT	i
TABLE OF CONTENTS	ii
LIST OF TABLES	iv
LIST OF FIGURES	v
NOMENCLATURES.....	vi
ABSTRACT	1
CHAPTER 1.....	2
INTRODUCTION.....	2
1.1 Background	2
1.2. Problem Description and Motivation	3
1.3. Objectives of the Study	4
1.4. Literature Review	4
1.5. Outline of the Thesis	7
CHAPTER 2.....	8
WIND ENERGY SYSTEMS AND WIND RESOURCES	8
2.1. Historical Uses of Wind	8
2.2. Wind Energy Conversion System	9
2.2.1. Wind Turbines.....	10
2.2.2. Wind Turbines Power Regulation Systems.....	13
2.2.3. Wind Turbine Generators.....	14
2.3. Wind Turbines Efficiency and Power Curve	15
2.4. Wind Energy Resources	16
2.4.1. Wind Speed Measurement	16
2.4.2. Wind Energy Resources Assessment in Ethiopia	18
2.5. Wind Power.....	20
2.5.1. Air Density	22
2.5.2. Swept Area	22
2.5.3. Wind Speed	23
2.5.4. Power Coefficient and Tip Speed Ratio.....	23
2.6. Wind Speed Distribution.....	24
2.6.1. Weibull Probability Distribution.....	24
SOLAR ENERGY SYSTEMS AND SOLAR ENERGY RESOURCES	27
3.1. Photovoltaic Power System.....	27
3.1.1. History of Photovoltaics.....	28
3.1.2. Photovoltaics Technology	28
3.2. PV Module and Array	31
3.3. Equivalent Electrical Circuit of PV Cell	31
3.4. I-V and P-V Curves.....	33
3.5. Solar Energy Resources	34
CHAPTER 4.....	37
DIESEL GENERATOR, BATTERY, AND POWER CONDITIONING UNITS.....	37
4.1. Diesel Generator.....	37

4.2. Battery	39
4.3.1. Charge Controller	40
4.4. Inverter	40
CHAPTER 5.....	42
HYBRID POWER GENERATION SYSTEM.....	42
5.1. Designing and Modeling of Hybrid System with HOMER	44
5.1.1. Simulation	45
5.1.2. Optimization.....	47
5.1.3. Sensitivity Analysis.....	48
5.1.4. Hybrid System Modeling	48
CHAPTER 6.....	66
RESULTS AND CONCLUSIONS	66
6.1. Results and Discussions	66
6.2. Conclusion.....	78
6.3. Recommendations	79
7. References	80
8. Appendix A: Overall Optimization Results Table	84

LIST OF TABLES

<i>Table 2.1: Monthly average wind speed (m/s)</i>	17
<i>Table 2.2: Friction Coefficient α of Various Terrains [Patel, 2006]</i>	18
<i>Table 2.3: Typical Shape Factor Values</i>	26
<i>Table 5.1: Monthly average daily electrical energy consumption (kWh)</i>	52
<i>Table 5.2: Inputs to the HOMER software</i>	64
<i>Table 6.1: Overall optimization results</i>	68
<i>Table 6.2: The first few lines of the optimization results for a diesel price of \$1.20</i>	71
<i>Table 6.3: optimization results in a Categorized form</i>	72
<i>Table 6.4: System report for the 84 % renewable resource contribution</i>	73
<i>Table 6.5: System report for the 83 % renewable resource contribution</i>	74
<i>Table 6.6: System report for the 96% renewable resource contribution</i>	75
<i>Table 6.7: System report for the 100% renewable resource contribution</i>	76
<i>Table 8.1: Overall optimization results</i>	84

LIST OF FIGURES

Figure 2.1: Block diagram of wind energy conversion system [Wang, 2006].....	9
Figure 2.2: Horizontal Axis Wind Turbines (HAWT) [Wind Powering America, 2010]	11
Figure 2.3: Vertical Axis Wind Turbines VAWT [World of Energy, 2007]	12
Figure 2.4: Power curve for HY-5 wind turbine [Hulk Energy, 2011]	15
Figure 2.5: Software generated monthly average wind speeds (at 2 m height)	20
Figure 2.6: An air parcel moving towards a wind turbine [Mathew, 2006].....	21
Figure 3.1: Basic structure of a generic silicon PV cell [Patel, 2006]	29
Figure 3.2: A PV cell equivalent electrical circuit [Duffie and Beckman, 2006]	32
Figure 3.3: I-V Curve of a typical silicon PV [Tzanakis, 2006]	33
Figure 3.4: P-V characteristic of the PV cell [Patel, 2006].....	34
Figure 4.1: Schematic of Diesel generator with constant engine speed [Leake, 2010]	37
Figure 4.2: The typical fuel curve of diesel generator [Leake, 2010]	38
Figure 5.1: General schemes for the standalone hybrid power supply system	43
Figure 5.2: HOMER diagram for the hybrid system.....	45
Figure 5.3: Primary load profile of the community	52
Figure 5.4: Monthly average deferrable load profiles.....	52
Figure 6.1: Monthly average wind resources	66
Figure 6.2: Monthly average solar resources	67
Figure 6.3: Contribution of the power units with 84 % RF, 1 st row in Table 6.1	69
Figure 6.4: Contribution of the power units with 83 % RF, 2 nd row in Table 6.1	70
Figure 6.5: Contribution of the power units with 96 % RF.....	70
Figure 6.6: Contribution of the power units with 100 % RF, bottom row of Tab. 6.1	71
Figure 6.7: Cost summary for the 84 % renewable resource contribution.....	73
Figure 6.8: Cost summary for the 83 % renewable resource contribution.....	74
Figure 6.9: Cost summary for the 96 % renewable resource contribution.....	75
Figure 6.10: Cost summary for the 100% renewable resource contribution.....	76
Figure 6.11: Sensitivity of PV cost to diesel price with some important NPCs labeled.....	77

NOMENCLATURES

A	Cross sectional area	(m ²)
<i>ac</i>	<i>Alternating current</i>	
CDF	<i>Cumulative Density Function</i>	
COE	Cost of energy	(\$/kW)
<i>C_p</i>	The power coefficient	
C	the Weibull scale factor	(m/s)
<i>c</i>	The chord (width) of the blade	(m)
<i>c_{fuel,eff}</i>	The effective price of fuel	(\$/L)
<i>c_{om,gen}</i>	The O& M cost	(\$/hr)
<i>C_{rep,batt}</i>	Replacement cost of the battery bank	(\$)
<i>C_{rep,gen}</i>	The replacement cost	(\$)
D	the rotor diameter	(m)
<i>dc</i>	<i>Direct current</i>	
DC	<i>Duration Curve</i>	
F	fuel consumption in this hour	(l)
<i>F₀</i>	Generator fuel curve intercept coefficient	(l/hr/kW _{rated})
<i>F₁</i>	Generator fuel curve slope	(l/hr/kW)
<i>f</i>	The line frequency	(Hz)
<i>f_{PV}</i>	The PV derating factor	(%)
<i>G_{sc}</i>	The solar constant =1367	(W/m ²)
$\overline{G}_{T,STC}$	The incident radiation at standard test conditions =1000	(W/m ²)
\overline{H}	The monthly average daily radiation on a horizontal surface	(MJ/m ²)
HOMER	<i>Hybrid Optimization Model for Energy Renewables</i>	
\overline{H}_0	The monthly average daily extraterrestrial radiation on a horizontal surface	(MJ/m ²)
<i>h₁</i>	The reference height	(m)
I	Load current	(A)

I_D	Diode current	(A)
I_{Sh}	Shunt resistance current	(A)
I_L	photo-current produced by the cell	(A)
I_o	Reverse saturation current of diode	(A)
KE	The kinetic energy of a stream of air	(J)
K	Boltzmann's constant	
k	The Weibull shape factor	
M	Number of data points (Eq. 3.10)	
m	Mass of air parcel	(kg)
NPC	<i>Net present cost</i>	(\$)
N	the rotational speed of the rotor	(RPM)
N_{batt}	Number of batteries in the battery bank	
n_s	The synchronous speed	(RPM)
\bar{n}	Monthly average daily number of hours of bright sunshine	
P	Power	(W)
PDF	<i>Probability Density Function</i>	
pH	<i>pico-hydro</i>	
P_{gen}	Output of the generator in this hour	(kW)
P_{PV}	The power output of the PV array	(kW)
p	Air pressure	(Pa)
q	Charge on an electron	(C)
$Q_{lifetime}$	Lifetime throughput of a single battery	(kWh)
Q_{thrpt}	Annual battery throughput	(kWh/yr)
RF	<i>Renewable fraction</i>	
RPM	<i>Revolution per minute</i>	
R	Specific gas constant	(Jkg ⁻¹ K ⁻¹)
r	The radius of the rotor (Eq. 2.1)	(m)
R_{batt}	Battery bank life	(yr)
$R_{batt,f}$	Battery float life	(yr)

R_{gen}	The generator lifetime	(hr)
R_{sh}	The shunt resistance	(ohm)
T	Temperature	(°K)
T_c	The PV cell temperature in the current time step	(°C)
V	Wind speed (velocity)	(m/s)
V_{ref}	Reference speed	(m/s)
V_{oc}	The open-circuit voltage	(V)
v	The volume of air parcel	(m ³)
Y_{gen}	Rated capacity of generator	(kW)
Y_{PV}	The rated capacity of PV array	(kW)
Z	Height above ground level for the desired speed	(m)
Z_o	Roughness length in the current wind direction	(m)
Z_{ref}	Reference height	(m)
z	The number of the blades	
Z'	Elevation	(m)
α_p	The temperature coefficient of power	(%/°C)
σ	The solidity of the turbine	
α	Ground surface friction coefficient	
ρ	The density of air	(kg/m ³)
ρ_j	The j th readings of the air density	(kg/m ³)
λ	The tip speed ratio	
Ω	The angular velocity	(rad/s)
ϕ	The latitude of the location	(°)
δ	The declination angle	(°)
ω_s	The sunset hour angle	(°)
η_{rt}	Battery roundtrip efficiency	(%)

ABSTRACT

This thesis presents the design of a hybrid electric power generation system utilizing both wind and solar energy for supplying model community living in Ethiopian remote area. The work was begun by investigating wind and solar energy potentials of the desired site, compiling data from different sources and analyzing it using a software tool.

The data regarding wind speed and solar irradiation for the site understudy are collected from the National Metrological Agency (NMA) and analyzed using the software tool HOMER. The results related to wind energy potential are given in terms of the monthly average wind speed, the wind speed PDF, the wind speed CDF, the wind speed DC, and power density plot for the site. Whereas the solar energy potential, has been given in the form of solar radiation plots for the site. According to the results obtained through the analysis, the site has abundant solar energy potential and the wind energy potential is unquestionably high enough to be exploited for generating electric energy using wind turbines with low cut-in wind speed.

The design of a standalone PV-wind hybrid power generating system has proceeded based on the promising findings of these two renewable energy resource potentials, wind and solar. Electric load for the basic needs of the community such lighting, water pumping, a radio receiver, flour mill and medical equipment for a health clinic has been suggested. The simulations and design has been carried out using the HOMER software.

By running the software the simulation results which are lists of power supply systems have been generated and arranged in ascending order according to their net present cost. Sensitivity variables, such as range of wind speed, solar radiation, PV panel price and diesel price have been defined as inputs into the software and the optimization process has been carried out repeatedly for the sensitivity variables and the results have been refined accordingly.

Keywords: hybrid renewable energy system, wind energy, photovoltaic, HOMER, PV-wind hybrid, standalone system

CHAPTER 1

INTRODUCTION

1.1 Background

It is a well known fact that in many developing countries and less developed countries, a significant proportion of the population lives without usable electrical power. Ethiopia is one of developing countries with more than 80% of its population live without usable electricity [CIA, 2010]. The more noticeable benefits of usable electric power include: improved health care, improved education, better transportation systems, improved communication systems, a higher standard of living, and economic stability. Unfortunately, many of the rural areas of Ethiopia have not benefited from these uses of electricity in the same proportion as the more populated urban areas of the country. A major limitation to the development of many rural communities has been the lack of this usable electricity. Due to the remote location and the low population densities of the rural communities the traditional means of providing power has proven too expensive, undependable, difficult to maintain, and economically unjustifiable. Consequently, many of these communities remain without electricity and may never receive grid power from the utility.

The small town of Bulbul and surrounding communities (05:03N, 039:030E) are one of those rural areas which have no access to electricity. The remote location and the small size of this town made it impractical to electrify with traditional diesel power plants. The system of sole central diesel power plants have shown to require high maintenance, use large quantities of fuel, pollute the environment, and have a low level dependability. Consequently, a central diesel plant was not considered for this area. The community with school and health clinic requires electricity for lighting, refrigeration, medical tools, communication equipment, water pumping, sterilization, ceiling fan, medical and night education, etc.

A hybrid PV-wind power generation system is proposed to supply electricity to model community of 100 households which have a health clinic and school. The Hybrid Renewable

Power Generation System (HRPGS) is a system aimed at the production and utilization of the electrical energy coming from more than one source, provided that at least one of them is renewable [Gupta et al., 2008]. Such a system often includes some kind of storage in order to satisfy the demand during the periods in which the renewable sources are not available and to decrease the time shift between the peak load and the maximum power produced and power conditioning unit and controller to convert and control one form of energy to other.

1.2. Problem Description and Motivation

Most of the remote rural areas of Ethiopia are not yet electrified. Electrifying these remote areas by extending grid system to these rural communities is difficult and costly. As the current international trend in rural electrification is to utilize renewable energy resources; solar, wind, biomass, and micro hydro power systems can be seen as alternatives. Among these, wind and solar energy systems in stand-alone or hybrid forms are thought to be ideal solution for rural electrification due to abundant solar radiation and significant wind distribution availability nearby the rural community in Ethiopia.

Ethiopia lies in the sunny belt between northern latitudes of 3° and 15°, and thus the potential benefits of renewable energy resources such as solar and wind energy can be considerable. As mentioned in [Mulugeta, 1999] the total annual solar radiation reaching the territory is of the order of over 200 million tone oil equivalent (toe) per year, over thirteen fold the total annual energy consumption in the country. In terms of geographical distribution, solar radiation that reaches the surface increases as one travels from west to east: the insolation period is approximately 2200 hours of bright sunshine per year in the west increasing to over 3300 hours per year in the eastern semi-arid regions.

The same author mentioned in [Mulugeta, 1999] that the total wind resource potential across Ethiopia amounts to 42 million toe per year, which also exceeds gross energy consumption by about three fold. Temporal and spatial variations in wind resource distribution over Ethiopia are significant, with the most attractive sites located toward the eastern and northern regions where average annual wind speed typically exceeds 3.5 ms⁻¹.

So far, these vast renewable energy resources are not exploited sufficiently in the country, primarily due to the lack of scientific and methodological know-how as regards planning, site selection, and technical implementation. A further constraint prohibiting their utilization is that the real potential of these resources is not well-known, partly because of the lack of research emphasis in developing these technologies, and partly because of the insufficient resource data base.

Thus, in this thesis a hybrid renewable power generation system integrating these vast solar and wind resources is designed and modeled, to electrify the community living in Bulbul and area surrounding it.

1.3. Objectives of the Study

The primary objective of this thesis work is to design, and model a stand-alone PV-wind hybrid power generation system for Bulbul and surrounding areas.

Specific objectives

- Studying the solar and wind energy potential for south-eastern Ethiopian remote areas,
- Estimating loads for Bulbul and surrounding community,
- Designing hybrid renewable energy system for the community in Bulbul,
- Modeling hybrid renewable energy system for the community in Bulbul, and
- State the findings and give recommendations if any.

1.4. Literature Review

To get a better insight about the different energy sources, solar and wind energy potentials of Ethiopian, hybrid power generation system, and rural electrification, an elaborated literature study was essential. Under the literatures study, the general introduction about the thesis on hybrid power system is described in Chapter 1. Chapter 1 to Chapter 4 and some of the first sections of Chapter 5 are descriptions made as a literature study.

Several researchers have been working in the area of standalone hybrid system since long time and numerous research results for a variety of applications have been published. In the following paragraphs some of papers reviewed are presented.

In [Nfah et al., 2010] a comparison between PV hybrid system (PVHS), standalone PV (SPV) and standalone diesel generator options have been performed using the net present value (NPV) technique. The authors consider a typical village mini-grid energy demand of 7.08 kWh/day in the computations of energy costs. For computation they conducted two sensitivity analyses. In the first sensitivity analysis a PV module price is fixed at 7.5 €/Wp and the remote diesel prices of 0.8 €/l, 0.98 €/l, 1.12 €/l, and 1.28 €/l are used. The energy cost for this option was found to be 0.812 €/kWh at a diesel price of 1.12 €/l.

The second sensitivity analysis is conducted using PV module prices of 5.25 €/Wp, 6.75 €/Wp, 7.5 €/Wp with a remote diesel price of 1.12 €/l. In this sensitivity analysis the energy costs were found to be in the ranges 0.692-0.785 €/kWh. The sensitivity analysis showed that minimum energy costs were attained in PVHS at renewable fraction (RF) in the range of 82.6-95.3%.

In [Nfah et al., 2008] the authors performed simulation of off-grid generation options for remote villages for a load of 110 kWh/day and 12 Wp. In the research HOMER is used to simulate the energy cost of the different design options. The study is conducted based on solar and hydropower resources of the site. Using load data to which an hourly and daily noise of 5 % is added and also based on hydro and solar resources data, the levelized costs of energy for different renewable energy options have been calculated and the levelized cost of energy was found to be 0.296 €/kWh. This cost is for a micro-hydro hybrid system comprising a 14 kW micro-hydro generator, a 15 kW LPG (liquefied petroleum gas) generator and 36 kWh of battery storage.

In another simulation comprising of photovoltaic (PV) hybrid systems, an 18 kWp PV generator, a 15 kW LPG generator and 72 kWh of battery storage the levelized cost was also found as 0.576 €/kWh for remote petrol price of 1 €/l and LPG price of 0.70 €/m³. The authors

concluded that both simulation options prove to be the cheapest depending on where the location is within the country.

In [Kanase-Patil et al., 2010] authors studied off-grid electrification of seven villages in the Almora district of Uttarakhand state, India. The authors considered four different scenarios during modeling and optimization of integrated renewable energy systems to ensure reliability parameters such as energy index ratio and expected energy not supplied. In the study, biomass, solar, hydro and wind energy sources were considered and analyzed using LINGO and HOMER softwares. The optimum system reliability, total system cost and cost of energy (COE) have also been worked out by introducing the so called customer interruption cost.

In [Nfah and Ngundam, 2009] a pico-hydro (pH) and PV hybrid systems incorporating a biogas generator have been simulated for remote village in Cameroon using a load of 73 kWh/day and 8.3 kWp. HOMER was used for simulation of renewable energy systems. The load profile of a hostel in Cameroon, the solar insolation of the site and the flow of river Mungo are used as input for simulation. Assuming a 40% increase in the cost of imported power system components, the cost of energy was found to be either 0.352 €/kWh for a 5 kW pico-hydro generator with 72 kWh storage or 0.396 €/kWh for a 3 kWp photovoltaic generator with 36 kWh battery storage.

In [Celik, 2002] the author conducted a techno-economic analysis based on solar and wind biased months for autonomous hybrid PV/wind energy system. He has observed that any optimum combination of the hybrid PV/wind energy system provides higher system performance than either of the single systems for the same system cost for every battery storage capacity. The author has also observed that the magnitude of the battery storage capacity has important bearing on the system performance of single photovoltaic and wind systems.

1.5. Outline of the Thesis

This thesis is organized into six chapters. The first chapter introduces background of standalone hybrid power generation system, problem statement and motivation, objectives of the study, and literature review.

In chapter two, the basic background theory related to wind energy systems and wind energy resources are presented. Besides, the wind energy potential of the area is assessed. Chapter three covers the basic background related to solar energy systems and solar energy resources. In this chapter, discussions are made regarding the sun as a source of energy, the PV power systems and technologies, the determination of solar radiation from sunshine duration data, with the utilization of empirical formulas derived from different authors involving regression coefficients. In chapter four the theories concerning auxiliary components of the hybrid system such as diesel generation, battery banks and inverters are described.

Hybrid system designing and modeling are presented in chapter five. In this chapter the software tool used for this work is thoroughly discussed. Finally, chapter six presents results of the thesis, conclusions drawn and recommendations made.

CHAPTER 2

WIND ENERGY SYSTEMS AND WIND RESOURCES

Wind is the movement of air caused by pressure differences within the atmosphere. This pressure differences exert a force that causes air masses to move from a region of high pressure to one of low pressure. That movement of air is referred as wind. Such pressure differences are caused primarily by uneven heating effects of the sun on the Earth's surface. Thus, wind energy is form of solar energy [Breeze et al., 2009]. Wind power is the transformation of wind energy into more utilizable forms, typically electricity using wind turbines.

The wind turbine captures the wind's kinetic energy of air mass by a rotor consisting of two or more blades which is mechanically coupled to an electrical generator. Most of the time the turbine is mounted on a tall tower to enhance the energy capture. The sites with steady high wind produce more energy over the year [Patel, 2006].

2.1. Historical Uses of Wind

Wind energy is one of the oldest sources of energy used by humankind, comparable only to the use of animal force and biomass [Wagner and Mathur, 2009]. Some 5000 yr ago wind was used to sail ships in the Nile. Many civilizations used wind power for transportation and other purposes: The Europeans used it to accomplish some mechanical works such as grind grains and pump water in the 1700s and 1800s. The first wind turbine used to generate electricity was installed in U.S in 1890 [Patel, 2006]. However, for much of the twentieth century there was small interest in using wind energy other than for battery charging for distant dwellings. These low-power systems were quickly replaced once the electricity grid became available. The sudden increases in the price of oil in 1973 stimulated a number of research, development and demonstrations of wind turbines and other alternative energy technologies in different countries [Rivera, 2008].

Ethiopia has not used its wind energy potential yet. However, some mechanical applications such as water pumping are being used in Rift valley areas. In the Zuway region alone, 67 wind pumps provide drinking water for more than 120,000 people [Bimrew, 2007].

2.2. Wind Energy Conversion System

The block diagram of a typical wind energy conversion system is shown in Figure 2.1 below.

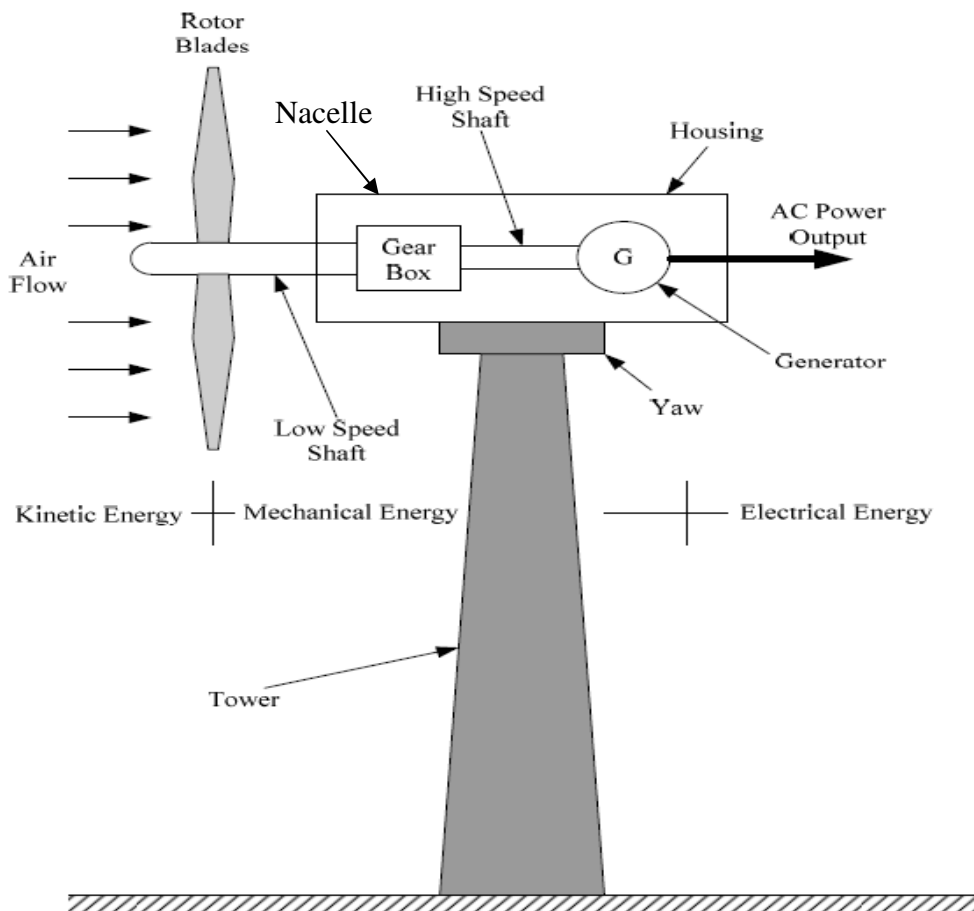


Figure 2.1: Block diagram of wind energy conversion system [Wang, 2006].

A modern wind turbine comprises of the principal components such as the tower, the yaw, the rotor and the nacelle, which houses the gear box and the generator. The tower holds the main part of the wind turbine and keeps the rotating blades at a height to capture sufficient wind power. The yaw mechanism is used to turn the wind turbine rotor blades in direction of the

wind. The gearbox transforms the slower rotational speeds of the wind turbine to higher rotational speeds on the electrical generator side. Electrical generator will generate electricity when its shaft is driven by the wind turbine, whose output is maintained as per specifications, by employing suitable control and supervising techniques [Patel, 2006].

2.2.1. Wind Turbines

Wind turbines are mechanical devices specifically designed to convert part of the kinetic energy of the wind into mechanical energy. If the mechanical energy is directly used by machinery, such as pumping water or grinding stones, the machine is called a windmill. If the mechanical energy is then converted to electricity, the machine is called a wind generator. Several designs of wind turbines have been devised throughout the times. Most of them comprise a rotor that turns round propelled by lift or drag forces, which result from its interaction with the wind. Depending on the position of the rotor axis, wind turbines are classified into vertical-axis and horizontal-axis ones [Fernando et al., 2007].

Based on a non-dimensional value known as the tip speed ratio (λ), which is defined as the ratio of the speed of the extremities of a wind turbine rotor to the speed of the free wind, modern wind turbines are also classified as high rotation speed ones and low rotation speed ones. This ratio can be taken as a metric in comparing the different characteristics of the wind turbines.

Solidity is other parameter, which is used to distinguish wind turbines. It is usually defined as the percentage of the area of the rotor, which contains material rather than air.

For horizontal axis machines it is defined as [Tzanakis, 2006]:

$$\sigma = \frac{z \cdot c \cdot r^2}{\pi r} \quad 2.1$$

For vertical axis machines it is defined as:

$$\sigma = \frac{z \cdot c}{r} \quad 2.2$$

where parameter σ is the solidity of the turbine, z is the number of the blades, r is the radius of the rotor and c is the chord (width) of the blade.

2.2.1.1. Horizontal Axis Wind Turbines

The axis of rotation of horizontal axis wind turbines (HAWT) is horizontal to the ground and almost parallel to the wind stream (Figure 2.2). They can operate with the blades in front of the wind (up-wind) or behind the wind (down-wind). They have one, two, three or a large number of blades and they cover approximately 90% of the installed wind turbines around the world. Most of today's commercial wind machines are three blades HAWTs due to their aerodynamic stability.

Low cut-in wind speed, easy furling and high power coefficient are the distinct advantages of horizontal axis machines. However, the generator and gearbox of these turbines are to be placed over the tower which makes its design more complex and expensive. Another disadvantage is the need for the tail or yaw drive to orient the turbine towards wind [Mathew, 2006].



Figure 2.2: Horizontal Axis Wind Turbines (HAWT) [Wind Powering America, 2010]

2.2.1.2. Vertical Axis Wind Turbines

The axis of rotation of vertical axis wind turbine (VAWT) is vertical to the ground and almost perpendicular to the wind direction as seen in Figure 2.3. The VAWT can receive wind from any direction. Hence complicated yaw devices can be eliminated. Vertical axis machines have very good aerodynamic efficiency and have low manufacture cost and simple control systems. The generator and the gearbox of such systems can be housed at the ground level, which makes the tower design simple and more economical. Moreover the maintenance of these turbines can be done at the ground level.

The major drawback of VAWT is that they are usually not self starting. So, additional mechanisms are required to ‘push’ and start the turbine, once it is stopped. There are chances that the blades may run at dangerously high speeds causing the system to fail, if not controlled properly. Further, guy wires are required to support the tower structure which may pose practical difficulties.



Figure 2.3: Vertical Axis Wind Turbines VAWT [World of Energy, 2007]

2.2.2. Wind Turbines Power Regulation Systems

All wind turbines are designed with some sort of power control. There are different ways to control aerodynamic forces on the turbine rotor and thus to limit the power in very high wind speeds in order to avoid damage to the turbine [Wind Turbines, 2011]. There are three commonly used types of power control in the industry.

- Stall Control
- Pitch Control
- Active stall regulation

The simplest, most robust and cheapest control method is the stall control (also called passive control), where the blades are bolted onto the hub at a fixed angle. The fixed-blade pitch is chosen so that the turbine reaches its maximum or rated power at the desired wind speed. The design of the rotor aerodynamics causes the rotor to stall (lose power) when the wind speed exceeds a certain level which limits the aerodynamic power on the blades.

Another type of control is pitch control, where the blades can be turned out or into the wind as the power output becomes too high or too low, respectively. Generally, the advantages of this type of control are good power control, increased energy capture, assisted startup and emergency stop. The pitch change system has to act rapidly. From an electrical point of view, good power control means that at high wind speeds the mean value of the power output is kept close to the rated power of the generator. The extra complexity arising from the pitch mechanism and the higher power fluctuations at high wind speeds can be mentioned as the demerits of this control scheme.

The third possible control strategy is the active stall control, in which the stall of the blade is actively controlled by pitching the blades. At low wind speeds, the blades are pitched similar to a pitch-controlled wind turbine, in order to achieve maximum efficiency. At high wind speeds, the blades go into a deeper stall by being pitched slightly into the direction opposite to that of a pitch-controlled turbine. The active stall wind turbine achieves a smoother limited power,

without high power fluctuations as in the case of pitch-controlled wind turbines. This control type has the advantage of being able to compensate variation in air density and inherits the advantages of both pitch and stall control mechanisms.

There are also other control mechanisms such as the use of ailerons (flaps) to alter the geometry of the wings or yawing to turn the rotor partly out of the wind to decrease power.

2.2.3. Wind Turbine Generators

The wind turbine generator converts mechanical energy to electrical energy. Wind turbine generators are a bit different, compared to other generating units ordinarily attached to the electrical grid. One reason is that the generator has to work with a power source (the wind turbine rotor) which supplies very fluctuating mechanical power (torque). The transmission system consists of the rotor shaft with bearings, brake(s), an optional gearbox, as well as a generator and optional clutches. There are two types of generator, synchronous and asynchronous. Synchronous generators are more expensive compared to asynchronous (induction) generators. Six-pole asynchronous generators are the most commonly used types.

The speed of the asynchronous generator varies with the turning force (torque) applied to it. It has a slightly softer connection to the network frequency than the synchronous generator, as it allows a limited amount of slip, or variation, in generator RPM.

In the case of the synchronous generator, the speed is set by the grid frequency and the number of pairs of poles of generators. The generator runs at a fixed frequency (line frequency), and hence at a fixed speed. Equation 2.3 gives the relationship between the frequency and the synchronous speed.

$$n_s = \frac{60f}{p'} \tag{2.3}$$

where n_s is the synchronous speed, f the line frequency and p' the number of pole pairs.

2.3. Wind Turbines Efficiency and Power Curve

Albert Betz, the German aerodynamicist, was derived the theoretical limit of power extraction from wind, or any other fluid. Betz law, states that 59% or less of the kinetic energy in the wind can be transformed to mechanical energy using a wind turbine. In practice, wind turbines rotors deliver much less than Betz limit. The efficiency of a turbine depends on different factors such as the turbine rotor, transmission and the generator. Normally the turbine rotors have efficiencies which vary from 40% to 50%. Gearbox and generator efficiencies can be estimated to be around 80% to 90%. Efficiency of turbine is not constant; it is function of wind speed. Many companies do not provide their wind turbine efficiencies rather the power curve of wind turbine is provided.

The power curve of a wind turbine is a graph that represents the turbine power output at different wind speeds values. The power curve is normally provided by the turbine's manufacture. Figure 2.4 presents an example of a wind turbine power curve. Note that at speeds from 0 to 2m/s the power output is zero. This occurs because there is no sufficient kinetic energy in the wind to move the wind turbine rotor. Normally the manufactures provide a technical data sheet where the start up and cut-off wind speed of the turbine is given. In general lower start up wind speeds result in higher energy coming from the turbine. This is beneficial especially in area with low wind speed profile.

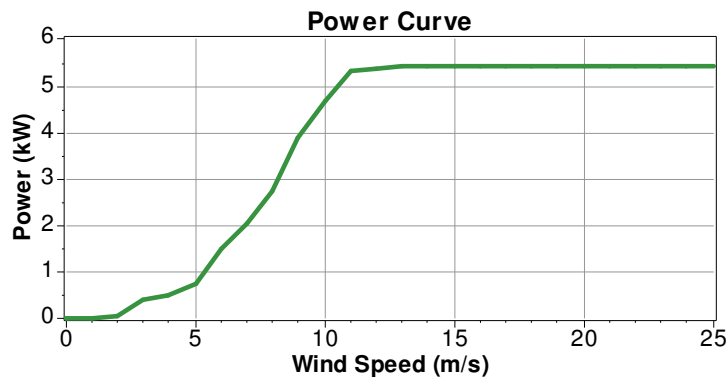


Figure 2.4: Power curve for HY-5 wind turbine [Hulk Energy, 2011]

2.4. Wind Energy Resources

Wind resource is the most important element in determining turbine performance at a given place. The energy that can be extracted from a wind stream is proportional to the cube of its velocity. In addition, the wind resource itself is intermittent. It varies with year, season, and time of day, elevation above ground, and form of terrain. Proper choice of site which is free from large obstructions, improves wind turbine's performance.

2.4.1. Wind Speed Measurement

2.4.1.1. Anemometer

The wind speed is measured with an instrument called an anemometer. These instruments come in several types. The most common type is a cup anemometer which has three or four cups attached to a rotating shaft. When the wind hits the anemometer, the cups and the shaft rotate. The angular speed of the spinning shaft is calibrated in terms of the linear speed of the wind. Normally, the anemometer is fitted with a wind vane to detect the wind direction. A data logger collects wind speed and wind direction data from the anemometer and wind vane respectively.

It is very important that the measuring equipment is set high enough to avoid turbulence created by trees, buildings or other obstructions. Readings would be most useful if they have been taken at hub height where the wind turbine is going to be installed [Gipe, 2004].

If the measurement of wind speed was not made at the wind turbine hub height (in this case it is 25 m) it is important to adjust the measured wind speed to the hub height. This can be done using either the logarithmic law, which assumes that the wind speed is proportional to the logarithm of the height above ground, or the power law, which assumes that the wind speed varies exponentially with height. Using the logarithmic law the wind speed at a certain height above ground level can be given as follows [Danish Wind, 2011]:

$$V = V_{ref} * \frac{\ln\left(\frac{Z}{Z_o}\right)}{\ln\left(\frac{Z_{ref}}{Z_o}\right)} \quad 2.4$$

where V is wind speed at height Z above ground level (m/s), V_{ref} is reference speed (m/s), i.e. a wind speed already known at height Z_{ref} , $\ln(\dots)$ is the natural logarithm function, Z is height above ground level for the desired speed (m), Z_o is roughness length in the current wind direction (m), and Z_{ref} is reference height (m), i.e. the height where we know the exact wind speed V_{ref} .

Table 2.1 summarizes the wind speed at 10 m and 25 m heights.

Table 2.1: Monthly average wind speed (m/s)

	Ja	Fe	Ma	Ap	Ma	Ju	Jul	Au	Se	Oc	No	De	Av.
At 10 m	3.7	4.0	3.8	3.1	3.7	4.5	5.2	4.9	4.3	3.4	3.4	4.0	4.0
At 25 m	4.4	4.8	4.6	3.7	4.4	5.3	6.4	5.9	5.2	4.1	4.1	4.4	4.4

Using power law the wind speed at a certain height above ground level can be given as follows [Patel, 2006]:

$$V_2 = V_1 \left(\frac{h_2}{h_1} \right)^\alpha \quad 2.5$$

Where: V_1 is wind speed measured at the reference height h_1 (m/s), V_2 is wind speed estimated at height h_2 (m/s), and α is ground surface friction coefficient.

Table 2.2: Friction Coefficient α of Various Terrains [Patel, 2006]

Terrain Type	Friction Coefficient α
Lake, ocean, and smooth, hard ground	0.10
Foot-high grass on level ground	0.15
Tall crops, hedges, and shrubs	0.20
Wooded country with many trees	0.25
Small town with some trees and shrubs	0.30
City area with tall buildings	0.40

2.4.2. Wind Energy Resources Assessment in Ethiopia

Several studies have been done regarding the wind energy potential in Ethiopia. From these studies those done by [Wolde-Ghiorgis W, 1988] and [Drake and Mulugetta, 1996] have given substantial results regarding the wind energy potential in the country by identifying the wind regimes in several areas. However, the data used in these studies is relatively old; the most recent data used in the first study is from 1968-1973 and was recorded only three times a day, at 6:00, 12:00, and 18:00. The remaining data used was also recorded three times a day at 8:00, 14:00 and 19:00 during the period 1937 – 1940.

Data used by [Drake and Mulugetta, 1996] was collected during the period 1979-1990 at 60 different locations across the country and recordings were made, according to the author, 4 to 7 times per day at a height of 2 m.

In addition to these studies [Getachew, 2009] had conducted wind energy surveys on four sites in the country. His study focuses on four specific locations, carefully selected in such a way that they represent a significant portion of the habitable parts of the country. Data used in this study was collected during the period 2000-2003, according to author recordings were made five times daily, at 6:00, 9:00, 12:00, 15:00, and 18:00, at a height of 10 meters.

Unlike the previous studies, this study focuses on one specific location called Bulbul situated in south-eastern part of the country.

2.4.2.1 The Wind Energy Potential

Compared to the previous studies, the data used in this work is relatively recent, from 2003 – 2005, and it is data which has been recorded over 24 hours using data logger attached to cup anemometer, at a height of 2 meters, for three consecutive years.

NMA collects wind speed and direction data using various types of Lambrecht cup anemometer and records on data logger attached to it. The wind vane, which is used to measure wind direction, is integrated with the instrument. The cup and wind vane sensor are mounted on the same shaft. A disadvantage of cup anemometers is the so-called over-speeding caused by their nonlinear response to fluctuating winds once they gain momentum in windy conditions [Getachew, 2009].

The location investigated is Bulbul (05:03N, 039:030E), 1448 m. The data is collected from NMA. The data can be claimed to be fairly complete for the given period of time, with only few recordings missing here and there. The missing data has been replaced by the averages of the preceding and following readings. For verification purposes, data from other sources has been investigated for the site [NASA, 2010] and [SWERA, 2011].

HOMER software is used to analyze the data. More detail about HOMER is given in section 5.1.

The monthly average wind speed data measured over the three years is the principal parameter used by the software to synthesize the potential wind speed of the site. It is from this data the hourly data of a year (8760 hours) is synthesized.

Other data input into the software are given in section 5.2 in detail. These data with the shape parameter k , the anemometer height at which data is collected, the diurnal pattern strength, elevation of the location, the autocorrelation factor, etc are fed to the software.

The final result, i.e. the probable wind speed distribution or wind energy potential for the location is given in Figure 2.5.

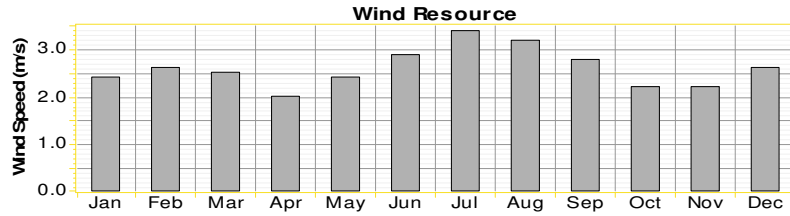


Figure 2.5: Software generated monthly average wind speeds (at 2 m height)

The potential of location has been evaluated against the wind power classification of the US Department of Energy (DOE). Accordingly the site potential is found to be of class 1 type. Class 1 potential is, in general, considered unsuitable for power generation [Getachew, 2009]. However, for off-grid electrical and mechanical applications such as battery charging and water pumping, average annual wind speed of 3 to 4 m/s may be adequate, which is certainly the purpose of this thesis work. Although the wind potentials may not be sufficient for independent wind energy conversion systems, it is believed that they are usable if integrated with other energy conversion systems such as PV, diesel generator and battery. The author of this work also believed that this wind energy potential can be exploited using wind turbines with low cut-in wind speed.

2.5. Wind Power

Energy available in wind is basically the kinetic energy of large masses of air moving over the Earth's surface. Blades of the wind turbine receive this kinetic energy, which is then transformed to useful mechanical energy, depending on end use [Mathew, 2006].

The kinetic energy of a stream of air with mass m (kg) and moving with a velocity V (m/s) is given in joules by the following equation [Patel, 2006; Mathew, 2006]:

$$KE = \frac{1}{2}mV^2 \quad 2.6$$

A wind rotor of cross sectional area A in m^2 is exposed to this wind stream with velocity V in m/s as depicted in Figure 2.6 below. The kinetic energy of the air stream available for the turbine can be expressed as:

$$KE = \frac{1}{2} \rho v V^2 \quad 2.7$$

where ρ is the density of air (kg/m^3) and v is the volume of air parcel available to the rotor (m^3). The air parcel interacting with the rotor per unit time has a cross-sectional area equal to that of the rotor area (A_T) and thickness equal to the wind velocity (V). Hence energy per unit time, that is power in the wind, can be expressed as:

$$P = \frac{1}{2} \rho A_T V^3 \quad 2.8$$

From Eq. (2.8), we can see that the factors influencing the power available in the wind stream are the air density, area of the wind rotor and the wind velocity. Effect of the wind velocity is more prominent owing to its cubic relationship with the power.

The most accurate estimate for wind power density in W/m^2 is that given by equation (2.9) [Getachew, 2009].

$$P/A = \frac{1}{2} \cdot \frac{1}{n} \cdot \sum_{j=1}^n (\rho_j \cdot V_j^3) \quad 2.9$$

where n is the number of wind speed readings and ρ_j and V_j are the j^{th} readings of the air density (kg/m^3) and wind speed (m/s) respectively.

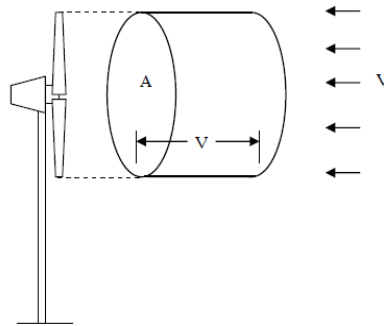


Figure 2.6: An air parcel moving towards a wind turbine [Mathew, 2006]

2.5.1. Air Density

Factors like temperature, atmospheric pressure, elevation and air constituents affect the density of air. Warm air in the summer is less dense than cold air in the winter. However at higher elevation the air is less dense than lower elevation. A density correction should be made for higher elevations and cooler weather. The air density ρ varies with pressure and temperature in accordance with the gas law as follows [Patel, 2006]:

$$\rho = \frac{P}{RT} \quad 2.10$$

where p is air pressure (Pa) and R is the specific gas constant ($287 \text{ Jkg}^{-1} \text{ K}^{-1}$) and T is air temperature in $^{\circ}\text{K}$. If we know the elevation Z' (m) and temperature T at a site, then the air density can be calculated by [Mathew, 2006]:

$$\rho = \frac{353.049}{T} e^{\left(-0.034 \frac{Z'}{T}\right)} \quad 2.11$$

If pressure and temperature data is not available, the following correlation may be used for estimating the density [Getachew, 2009]:

$$\rho = 1.225 - (1.194 * 10^{-4}) * Z' \quad 2.12$$

2.5.2. Swept Area

As shown in equation 2.7, the output power is also related to the area intercepting the wind, that is, the area swept by the wind turbines rotor. For the horizontal axis turbine, the rotor swept area is the area of a circle:

$$A = \frac{\pi}{4} D^2 \quad 2.13$$

where: D is the rotor diameter in meters. The relationship between the rotor's diameter and the energy capture is fundamental to understanding wind turbine design. Relatively small increases

in blade length or in rotor diameter produce a correspondingly bigger increase in the swept area, and therefore, in power. The wind turbine with the larger rotor will almost invariably generate more electricity than a turbine with a smaller rotor, not considering generator ratings [Gipe, 2004].

2.5.3. Wind Speed

As mentioned earlier the wind velocity is the most prominent factor for deciding the power available in the wind spectra due to its cubic relationship with power. Hence, in selecting the right site it plays a major role in the success of a wind power projects.

Using the average annual wind speed alone in the power equation would not give us the right results; the calculation would differ from the actual power in the wind by a factor of two or more. The reason for this number representing the average speed ignores the amount of wind above as well below the average. It is the wind speed above the average that contributes most of the power [Ramos, 2005].

2.5.4. Power Coefficient and Tip Speed Ratio

Theoretical power available in a wind stream is given by Eq. (2.8). However, a turbine cannot extract this power completely from the wind. When the wind stream passes the turbine, a part of its kinetic energy is transferred to the rotor and the air leaving the turbine carries the rest away. Actual power produced by a rotor would thus be decided by the efficiency with which this energy transfer from wind to the rotor takes place. This efficiency is usually termed as the power coefficient (C_p). Thus, the power coefficient of the rotor can be defined as the ratio of actual power developed by the rotor to the theoretical power available in the wind [Mathew, 2006; Wagner and Mathur, 2009].

$$C_p = \frac{P_{rotor}}{P_{mech}} \quad 2.14$$

where: P_{rotor} is the power developed by the rotor (W) and P_{mech} mechanical power in the wind (W). The power coefficient of a turbine depends on many factors such as the profile of the rotor blades, blade arrangement and setting etc.

The power developed by a rotor at a certain wind speed greatly depends on the relative velocity between the rotor tip and the wind. The ratio between the velocity of the rotor tip and the wind velocity is termed as the tip speed ratio (λ). Thus, the tip speed ratio can be given by the equation 2.15 [Mathew, 2006]:

$$\lambda = \frac{r\Omega}{V} = \frac{2\pi Nr}{V} \quad 2.15$$

where Ω is the angular velocity (rad/s), r is the radius of the blade (m), V is the wind velocity (m/s) and N is the rotational speed of the rotor (rpm). The power coefficient of a rotor varies with the tip speed ratio. There is an optimum λ for a given rotor at which the energy transfer is most efficient and thus the power coefficient is the maximum (CP max).

2.6. Wind Speed Distribution

Wind speed is the most critical data needed to appraise the power potential of a site due to its cubic relation with the power. The wind is never constant at any site. It is influenced by weather system, the local land terrain, and its height above the ground surface. Wind speed varies within the minute, hour, day, season, and even by year. Since wind velocity varies it is necessary to capture this variation in the model used to predict energy production. This is usually done using probability functions to describe wind velocity over a period of time [Patel, 2006].

2.6.1. Weibull Probability Distribution

A probability density function (PDF) best describes the variation in wind speed. A PDF is used to model the wind velocity variation. It provides the probability that an event will occur between two end points. The area under the curve between any two speeds greater than zero will equal the probability that wind will blow somewhere between those two speeds. The actual height

and shape of a PDF curve are determined such that the area under the curve from 0 to infinity is exactly 1. Physically, this means that there is a 100% chance that the wind will blow at some speed between 0 m/s and infinite m/s.

The Weibull probability distribution is a very accurate model in describing wind velocity variation as it conforms well to the observed long-term distribution of mean wind speeds for a range of sites [Rivera, 2008]. This PDF found in the literature using different notations. In this thesis the notations used in [Mathew, 2006] and [Patel, 2006] are adopted.

$$f(V) = \frac{k}{C} \left(\frac{V}{C}\right)^{k-1} \exp\left[-\left(\frac{V}{C}\right)^k\right] \quad \text{for } 0 < V < \infty \quad 2.16$$

where k is the Weibull shape factor, C is the scale factor (m/s) and V represents in this case the wind speed (m/s). For a given average wind speed, a smaller shape factor indicates a relatively wide distribution of wind speeds around the average while a larger shape factor indicates a relatively narrow distribution of wind speeds around the average. For $k = 2$ the Weibull PDF is commonly known as the Rayleigh density function. The PDF in this case become:

$$f(V) = \frac{2V}{C^2} \exp\left[-\left(\frac{V}{C}\right)^2\right] \quad 2.17$$

There are a number of ways to calculate the Weibull parameter. Some of them are: probability plots, least square parameter estimation, Maximum likelihood estimators, typical shape factors values, Justus Approximation, and the Quick Method [Ramos, 2005]. These techniques give good result when sufficient data are available. An alternative way is to use typical shape factors values. The shape factor will normally range from 1 to 3. These typical values are known from experience and multiple observations of sites where wind speed measurements have been taken. Table 2.3 shows typical values for the shape factor [Rivera, 2008].

Table 2.3: Typical Shape Factor Values

Types of Wind	Shape Factor k
Inland Winds	1.5 to 2.5
Coastal Winds	2.5 to 3.5
Trade Winds	3 to 4

Once k determined, the scale factor (C) can be calculated using the following equation 2.18 [Mathew, 2006]:

$$C = \frac{\bar{V}}{\Gamma\left(1 + \frac{1}{k}\right)} \quad 2.18$$

where \bar{V} is the average wind speed (m/s) value and Γ is the gamma function [Mathew, 2006]. The average wind speed can be estimated using the equation 2.19:

$$\bar{V} = \left(\frac{1}{n} \sum_{i=1}^n V_i^m \right)^{\frac{1}{m}} \quad 2.19$$

where V_i is the actual wind speed measurement at interval i , n is the total number of wind speed measurements, and $m = 1$ for arithmetic mean, $m = 2$ for root mean square, and $m = 3$ for cubic root cube.

Typical shape factor is used when the only data available are average wind speed.

CHAPTER 3

SOLAR ENERGY SYSTEMS AND SOLAR ENERGY RESOURCES

The sun is the largest energy source of life at the same time it is the ultimate source of all energy (except tidal and geothermal power), even the energy in the fossil fuels ultimately comes from the sun. The sun radiates 174 trillion kWh of energy to the earth per hour. In other words, the earth receives 1.74×10^{17} watts of power from the sun [Danish Wind, 2011].

The sun is a typical star with mass 2×10^{30} kg, beam length 700,000 km and it has roughly 5 billions more years of life. Its surface temperature is about 5800 Kelvin while the internal temperature is approximately 15 million Kelvin. This temperature derives from reactions which were based on the transformation of hydrogen to helium, the process called nuclear fusion, which produces high temperature of the sun and the continuous emission of large amounts of energy. It is calculated that for each gram of hydrogen that is converted to helium sun radiates energy equal to 1.67×10^5 kWh. The solar energy is emitted to the universe mainly by electromagnetic radiation. Approximately one-third of energy radiated from sun is reflected back. The rest is absorbed and retransmitted to the space while the earth reradiates just as energy as it receives and creates a stable energy balance at a temperature suitable for life.

There are normally two ways to generate electricity from sunlight: through photovoltaic (PV) and solar thermal systems. In this thesis, only photovoltaic power system will be discussed.

3.1. Photovoltaic Power System

Photovoltaic (PV) is a method of generating electrical power by converting solar radiation into direct current electricity using semiconductors that exhibit the photovoltaic effect. PV power generation uses solar panels comprising a number of cells containing a semi-conducting material. As long as light is shining on the solar cell, it generates electrical power. When the light stops, the electricity stops. Many PV have been in continuous outdoor operation on Earth or space for over 30 yrs [Luque and Hegedus, 2003].

3.1.1. History of Photovoltaics

The history of photovoltaic was date back to 1839 when a French physicist Alexander Edmond Becquerel discovered the photovoltaic effect while experimenting with an electrolytic cell made up of two metal electrodes. When cells were exposed to light the generation of electricity increased. In 1877 the first report of PV effect was published by two Cambridge scientists Adams and Day and in 1883 Charles Fritts built a selenium solar cell similar to contemporary solar silicon cells with efficiency less than 1%. In 1954 Chapin, Fuller and Pearson announced the first manufacture of solar element in Bell Laboratory with p-n junction and efficiency 6%. The initial commercial manufactures were very costly, with relatively small efficiency of about 5-10% and they were made by crystalline materials, mainly by crystal silicon (c-Si).

The technology of photovoltaic cells was developed rapidly during the second half of the twentieth century. It soon found applications in U.S. space programs for its high power-generation capacity per unit weight. Since then it has been extensively used to convert sunlight into electricity for earth-orbiting satellites. In the past the PV cost was very high. For that reason, PV applications have been limited to remote locations not connected to utility lines. But with the declining prices in PV, the market of solar modules has been growing at 25 to 30% annually during the last yrs [Patel, 2006].

Nowadays the efficiency of the best crystalline silicon cells has reached 24% for photovoltaic cells used in aerospace technology and about 14-18% overall efficiency for those used for industrial and domestic use. While 40.7% cell efficiency is achieved using structure called a multi-junction solar cell [Renewable Energy World, 2010]. The cost of PV cell is around 2\$/Wp if they are purchased in large quantities [Hulk Energy, 2011].

3.1.2. Photovoltaics Technology

Figure 3.1 shows the basic PV cell structure. Metallic contacts are provided on both sides of the junction to collect electrical current induced by the impinging photons. A thin conducting mesh of silver fibers on the top surface collects the current and lets the light through. The spacing of

the conducting fibers in the mesh is a matter of compromise between maximizing the electrical conductance and minimizing the blockage of the light. Conducting-foil (solder) contact is provided over the bottom surface and on one edge of the top surface. In addition to the basic elements, several enhancement features are also included in the construction. For example, the front face of the cell has an antireflective coating to absorb as much light as possible by minimizing the reflection. The mechanical protection is provided by a cover glass applied with a transparent adhesive.

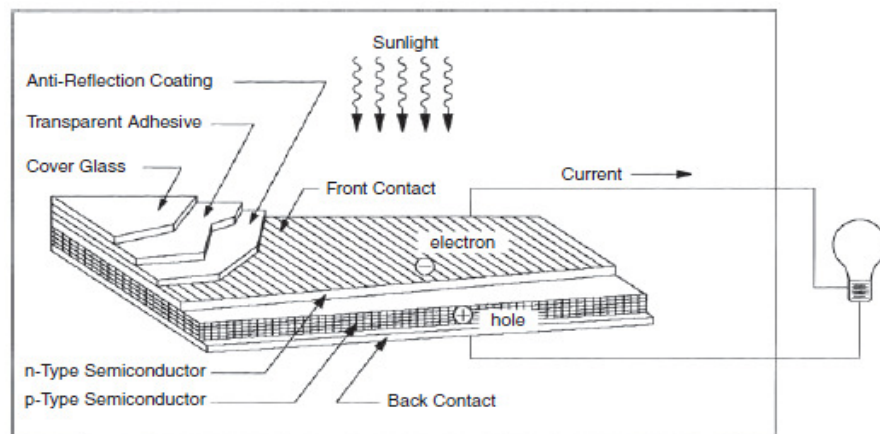


Figure 3.1: Basic structure of a generic silicon PV cell [Patel, 2006]

3.1.2.1. PV Cells

PV cells are made up of semiconductor material, such as silicon, which is currently the most commonly used element in semiconductor industry. Basically, when light strikes the cell, a certain portion of it is absorbed within the semiconductor material. When energy knocks semiconductor electrons loose, allowing them to flow freely. PV cells have one or more electric fields that act to force electrons that are freed by light absorption to flow in a certain direction. This flowing of electrons is a current and by placing metal contacts on the top and bottom of the PV cell we can draw that current off to be used externally. This current, together with the cell's voltage, which is a result of its built-in electric field or fields, defines the power in watts that the solar cell can produce [Patel, 2006].

3.1.2.1.1. Main PV Cell Types

The material that is used widely in the industry for the production of photovoltaic cells is silicon. Based on the structure of the basic material from which they are made and the particular way of their preparation the photovoltaic cells of silicon are categorized into four.

The types are the following ones:

1. **Single-Crystalline Silicon:** The basic material is mono-crystalline silicon. In order to make them, silicon is purified, melted, and crystallized into ingots. The ingots are sliced into thin wafers to make individual cells. It is the oldest and more expensive production technique, but it's also the most efficient and widely used sunlight conversion technology available. Cells efficiency oscillates between 14% and 18% [Patel, 2006].
2. **Polycrystalline or Multi-crystalline Silicon:** The particular cell is relatively large in size and it can be easily formed into square shape which virtually eliminates any inactive area between cells. It has a slightly lower conversion efficiency compared to single crystalline and manufacturing costs are also lower. Cells efficiency oscillates between 10% and 13% [Luque and Hegedus, 2003].
3. **String Ribbon:** This is a refinement of polycrystalline silicon production. There is less work in its production so costs are even lower. Cells efficiency averages 8% to 10%.
4. **Technology which uses thin film solar cells** while the total thickness of a semi conductor is about 1 μ m. Amorphous or thin film silicon cells are solids in which the silicon atoms are much less ordered than in a crystalline form. By using multiple junctions this kind of photovoltaic cells achieve maximum efficiency which is estimated at about 13% while the installation cost is reduced. The efficiency of this cell oscillates between 6% and 10% [Patel, 2006]. Furthermore the output of an amorphous silicon cell is not decreased as temperature increases and is much cheaper to produce than crystalline silicon.

Cells efficiency decreases with increases in temperature. Crystalline cells are more sensitive to heat than thin films cells. The output of a crystalline cell decreases approximately 0.5% with

every increase of one degree Celsius in cell temperature. For this reason modules should be kept as cool as possible, and in very hot condition amorphous silicon cells may be preferred because their output decreases by approximately 0.2% per degree Celsius increase [Patel, 2006, Luque and Hegedus, 2003].

3.2. PV Module and Array

The solar cell is the basic building block of the PV power system. However, it rarely used individually because it is not able to supply an electronic device with enough voltage and power. For this reason, many photovoltaic cells are connected in parallel or in series in order to achieve as higher voltage and power output as possible. Cells connected in series increases the voltage output while cells connected in parallel increases the current. The solar array or panel is a group of several modules electrically connected in series-parallel combination to generate the required current and voltage and hence the power.

A typical photovoltaic system is made of 36 individual 100cm² silicon photovoltaic cells and auxiliary devices which are lead-acid batteries with a typical voltage of 12 V. This system has the capacity of producing more than 13V during cloudy days and can charge a 12 V battery.

3.3. Equivalent Electrical Circuit of PV Cell

The complex physics of the PV cell can be represented by the equivalent electrical circuit shown in Figure 3.2 below. The following parameters call for consideration. The current I at the output terminals is equal to the light-generated current I_L , less the diode current I_D and the shunt-leakage current I_{sh} . The series resistance R_s represents the internal resistance to the current flow, and depends on the p-n junction depth, impurities, and contact resistance. The shunt resistance R_{sh} is inversely related to the leakage current to the ground. In an ideal PV cell $R_s = 0$ and $R_{sh} = \infty$. The PV conversion efficiency is sensitive to small variations in R_s , but insensitive to variations in R_{sh} . A small increase in R_s can decrease the PV output significantly.

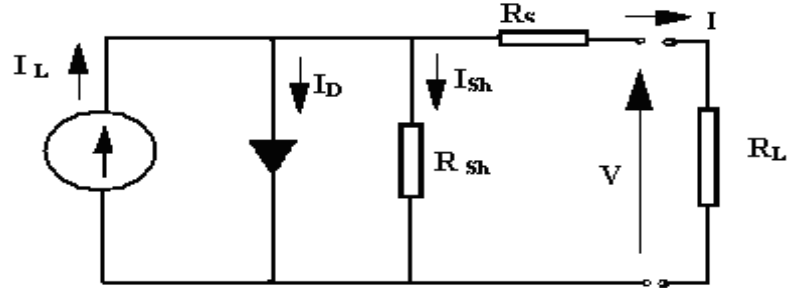


Figure 3.2: A PV cell equivalent electrical circuit [Duffie and Beckman, 2006]

The open-circuit voltage V_{oc} of the cell is obtained when the load current is zero and is given by the following:

$$V_{oc} = (I_L - I_D)R_{sh} \quad 3.1$$

The diode current is given by the classical diode current expression:

$$I_D = I_o \left[\exp\left(\frac{qV_{oc}}{AKT}\right) - 1 \right] \quad 3.2$$

where I_o is the saturation current of the diode (A), q is electron charge (1.6×10^{-19} C), A is curve-fitting constant, K is Boltzmann constant (1.38×10^{-23} J/°K), T is temperature on absolute scale °K.

Thus, the load current is given by the expression:

$$I = I_L - I_D - I_{sh}$$

$$I = I_L - I_o \left[\exp\left(\frac{qV_{oc}}{AKT}\right) - 1 \right] - \frac{V_{oc}}{R_{sh}} \quad 3.3$$

The last term is the leakage current to the ground. In practical cells, it is negligible compared to I_L and I_o and is generally ignored.

The two most important figure of merits widely used for describing PV cell electrical performance are the open-circuit voltage V_{oc} and the short-circuit current I_{sc} under full illumination. The short-circuit current is measured by shorting the output terminals and measuring the terminal current. Ignoring the small diode and ground leakage currents under zero voltage, the short-circuit current under this condition is the photocurrent I_L .

The maximum photo voltage is produced under the open-circuit voltage. Again by ignoring the ground leakage current, equation 3.3 with I give the open-circuit voltage as follows:

$$V_{oc} = \frac{AKT}{q} \ln\left(\frac{I_L}{I_o} + 1\right) \quad 3.4$$

3.4. I-V and P-V Curves

The electrical characteristic of the PV cell is generally represented by the current vs. voltage (I-V) curve. The figure below (Figure 3.3) depicts the I-V curve of typical PV cell. This curve shows the variation of current and voltage when cell resistance varies from zero to infinity. In this curve the point at which the voltage is zero is called the short-circuit current. This is the current we would measure with output terminal shorted. On the other hand the point at which current is zero is known as open-circuit voltage. This is the voltage we would measure with output terminal open. Somewhere in the middle of the two regions, the curve has a knee point.

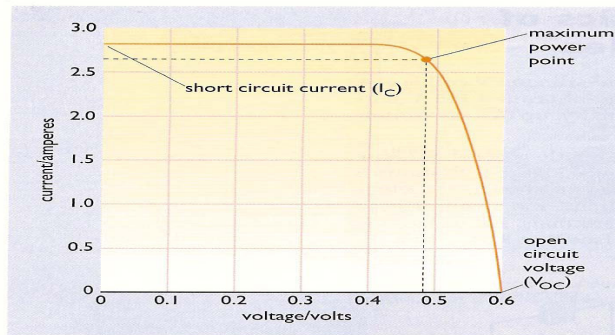


Figure 3.3: I-V Curve of a typical silicon PV [Tzanakis, 2006]

The power output of the panel is the product of the voltage and current outputs. In Figure 3.4, the power is plotted against the voltage which is P-V curve of the PV cell. Note that the cell produces no power at zero voltage or zero current, and produces the maximum power at the voltage corresponding to the knee point of the I-V curve. This is why the PV power circuit is always designed to operate close to the knee point with a slight slant on the left-hand side. The PV circuit is modeled approximately as a constant current source in the electrical analysis of the system.

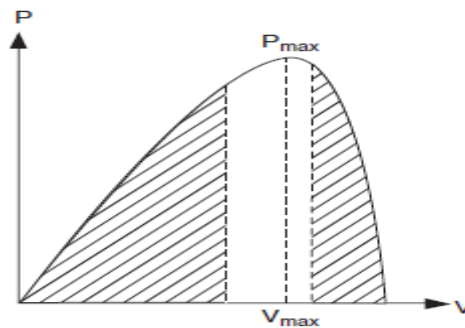


Figure 3.4: P-V characteristic of the PV cell [Patel, 2006]

Finally in order to measure the photovoltaic cells output power the following standard test conditions are established internationally. The irradiance level is 1000 W/m^2 , with the reference air mass 1.5 solar spectral irradiance distributions and cell or module junction temperature of 25°C .

3.5. Solar Energy Resources

Solar radiation provides a huge amount of energy to the earth. The total amount of energy, which is irradiated from the sun to the earth's surface, equals approximately 10,000 times the annual global energy consumption [Patel, 2006].

The light of the sun, which reaches the surface of the earth, consists mainly of two components: direct sunlight and indirect or diffuse sunlight, which is the light that has been scattered by dust and water particles in the atmosphere. Photovoltaic cells not only use the direct component of the light, but also produce electricity when the sky is overcast. To determine the PV electricity

generation potential for a particular site, it is important to assess the average total solar radiation received over the year. Unfortunately in most developing countries there is no properly recorded radiation data. What usually available is sunshine duration data.

Ethiopia is one of the developing countries which have no properly recorded solar radiation data and, like many other countries, what is available is sunshine duration data. However, given a knowledge of the number of sunshine hours and local atmospheric conditions, sunshine duration data can be used to estimate monthly average solar radiation, with the help of empirical equation 3.5 [Duffie and Beckman, 2006].

$$\bar{H} = \bar{H}_0 \left(a + b \left(\frac{\bar{n}}{N} \right) \right) \quad 3.5$$

where \bar{H} is the monthly average daily radiation on a horizontal surface (MJ/m²), \bar{H}_0 is the monthly average daily extraterrestrial radiation on a horizontal surface (MJ/m²), \bar{n} is the monthly average daily number of hours of bright sunshine, N is the monthly average of the maximum possible daily hours of bright sunshine, a and b are regression coefficients

Solar radiation, known as extraterrestrial radiation, H_0 , on a horizontal plane outside the atmosphere, is given by equation 3.6.

$$H_0 = \frac{24 * 3600 * G_{sc}}{\pi} \left(1 + 0.033 * \cos \left(\frac{360 n_d}{365} \right) \right) * \left(\cos \phi \cos \delta \sin \omega s + \frac{\pi \omega s}{180} \sin \phi \sin \delta \right) \quad 3.6$$

where n_d is the day number, G_{sc} is the solar constant (1367 W/m²), ϕ is the latitude of the location (°), δ is the declination angle (°), which is given as follows:

$$\delta = 23.45 \sin \left(360 \frac{248 + n_d}{365} \right) \quad 3.7$$

ω_s = the sunset hour angle ($^\circ$), which is given by equation 3.9 below:

$$\omega_s = \cos^{-1}(-\tan \phi \tan \delta) \quad 3.8$$

The maximum possible sunshine duration N is given by

$$N = \frac{2}{15} \omega_s \quad 3.9$$

Equations (3.6) and (3.9) are used to calculate the daily extraterrestrial radiation and the maximum possible daily hours of bright sunshine respectively at the specified location.

The regression coefficients a and b for M number of data points can be calculated from the following equations (3.10) and (3.11) respectively [Getachew, 2009].

$$a = \frac{\sum \frac{\bar{H}}{\bar{H}_0} \sum \left(\frac{\bar{n}}{\bar{N}} \right)^2 - \sum \frac{\bar{n}}{\bar{N}} \sum \frac{\bar{n}}{\bar{N}} \frac{\bar{H}}{\bar{H}_0}}{M \sum \left(\frac{\bar{n}}{\bar{N}} \right)^2 - \left(\sum \frac{\bar{n}}{\bar{N}} \right)^2} \quad 3.10$$

$$b = \frac{M \sum \frac{\bar{n}}{\bar{N}} \frac{\bar{H}}{\bar{H}_0} - \sum \frac{\bar{n}}{\bar{N}} \sum \frac{\bar{H}}{\bar{H}_0}}{M \sum \left(\frac{\bar{n}}{\bar{N}} \right)^2 - \left(\sum \frac{\bar{n}}{\bar{N}} \right)^2} \quad 3.11$$

Results estimated in this way are compared with the data which are obtained from sources such as NASA's surface solar energy data set or the SWERA global meteorological database. Drake and Mulugetta developed sets of constants a and b for various locations in Ethiopian [Drake and Mulugetta, 1996]. In this thesis, regression coefficients developed in their work was used.

The global solar radiation obtained using equation 3.5 is fed to HOMER software as input.

CHAPTER 4

DIESEL GENERATOR, BATTERY, AND POWER CONDITIONING UNITS

In the previous two chapters wind and solar energy systems and resources are thoroughly discussed. These two resources are the primary sources for the hybrid system studied in this thesis. Wind turbines and PV panels are the basic components for this hybrid system. In this chapter diesel generator, battery and power condition units, which are the ancillary components for the hybrid system are presented.

4.1. Diesel Generator

Diesel generator is one of the elements of hybrid system described in this thesis. A diesel generator is an engine which use diesel as the prime mover to generate electric energy. It supplies the load when there is less supply from renewable energy sources than demand for an efficient, continuous, and reliable customers' energy demand. The following figure, Figure 4.1, shows the schematic of a diesel generator.

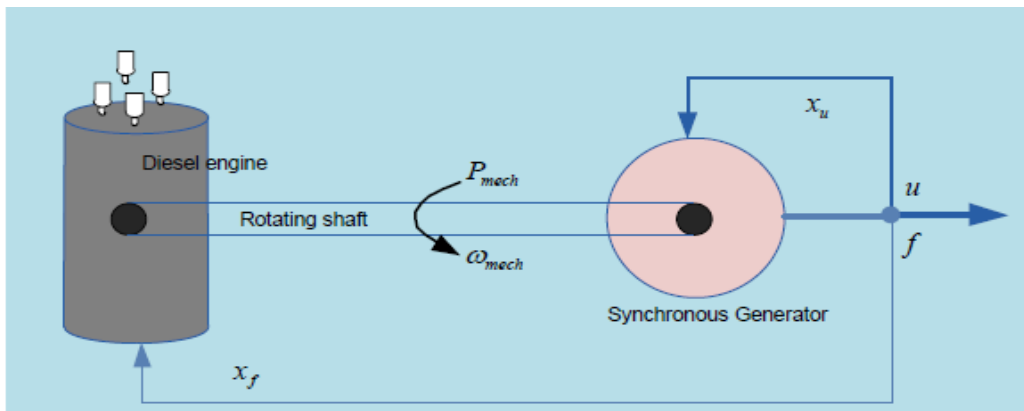


Figure 4.1: Schematic of Diesel generator with constant engine speed [Leake, 2010]

A synchronous type generator is used to produce ac-power when the unit's turbine is rotated by a prime mover coupled to the diesel engine shaft. It operates at constant speed of engine which

corresponds to the required generator output voltage frequency (50 Hz or 60 Hz). The synchronous generator must control its output voltage by controlling the excitation current. For this operation, the output voltage u is controlled by the control signal x_u and the speed of the engine and thus the frequency f is controlled by the control signal x_f . These types of diesel generators mostly operate at efficiency of about 30% for nominal load, and when they operate at lower portion of the nominal load, the efficiency further reduces. Generators of this type operating at lower capacity than the nominal load consume more relative fuel consumption than they can consume when operating at nominal load, as shown in Figure 4.2. Diesel generator-set has the following drawbacks.

- Very heavy and difficult to handle
- Noisy
- Low efficiency

As it can be observed from Figure 4.2, the diesel generator fuel consumption depends on the output power. About 25% of the fuel at rated full power is still consumed by the diesel generator even if no power is generated from it.

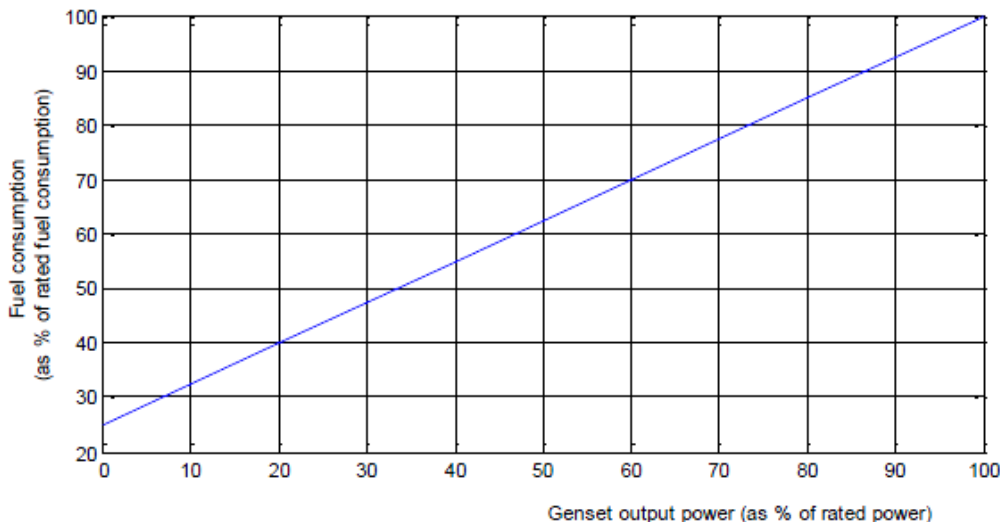


Figure 4.2: The typical fuel curve of diesel generator [Leake, 2010]

4.2. Battery

A battery is a device that stores direct current (dc) electrical energy in electrochemical form for later use. The amount of energy that will be stored or delivered from the battery is managed by the battery charge controller.

Electrical energy is stored in a battery in electrochemical form and is the most widely used device for energy store in a variety of application. The conversion efficiency of batteries is not perfect. Energy is lost as heat and in the chemical reaction, during charging or recharging. Because not all battery's can be recharged they are divided in two groups. The first group is the primary batteries which only converts chemical energy to electrical energy and cannot be recharged. The second group is rechargeable batteries. Rechargeable batteries are used in hybrid power generation system.

The internal component of a typical electrochemical cell has positive and negative electrodes plates with insulating separators and a chemical electrolyte in between. The cells store electrochemical energy at a low electrical potential, typically a few volts. The cell capacity, denoted by C, is measured in ampere-hours (Ah), meaning it can deliver C A for one hour or C*n A for n hours, [Luque and Hegedus, 2003].

Many types of batteries are available today, such as Lead-acid, Nickel cadmium, Nickel-metal, Lithium-ion, Lithium-polymer and Zinc air. Lead-acid rechargeable batteries continue to be the most used in energy storage applications because of its maturity and high performance over cost ratio, even though it has the least energy density by weight and volume. These lead acid batteries come in many versions. The shallow- cycle version is the one use in automobiles, in which a short burst of energy is drawn from the battery to start the engine. The deep-cycle version, on the other hand, is suitable for repeated full charge and discharge cycles. Most energy store applications require deep-cycle batteries [Patel, 2006].

Depth of discharge is import factor for the battery. It refers to how much capacity will be used from the battery. Most systems are designed for regular discharges of up to 40 to 80 percent.

Battery life is directly related to how deep the battery is cycled. For example, if a battery is discharged to 50 percent every day, it will last about twice long as if is cycled to 80 percent [Leake, 2010].

The main factors affecting battery lifetime are grid corrosion, buckling of plates, sulfation, and stratification of the electrolytes. These factors are causing loss of active material and internal short circuits. If less active materials available the ratio of the reaction components is becoming non-optimal resulting in a drop of capacity and the charging efficiency is reduced. Internal short circuit leads to harmful deep discharge of the concerned cell and hence ruins the whole battery.

Atmospheric temperature also affects the performance of batteries. Manufacturers generally rate their batteries at 25°C. The battery's capacity will decrease at lower temperatures and increase at higher temperature. The battery's life increases at lower temperature and decreases at higher. It is recommended to keep the battery's storage system at 25 °C.

4.3.1. Charge Controller

The battery charge controller works as a voltage regulator. The primary function of a charge controller is to prevent the battery from being overcharged by a generating unit system. A charge controller constantly monitors the battery's voltage. When the batteries are fully charged, the controller will stop or decrease the amount of current flowing from the generating system into the battery. The controllers average efficiencies range from 95% to 98% [Luque and Hegedus, 2003].

4.4. Inverter

An inverter converts the direct current (dc) electricity from sources such as batteries, PV modules, or wind turbine to alternative current (ac) electricity. The electricity can then be used to operate ac equipment like the ones that are plugged in to most house hold electrical outlets. The normal output ac waveform of inverters is a sine wave with a frequency of 50/60Hz.

Inverters are available in three different categories based on where they are applied: grid-tied battery less, grid tied with battery back-up and stand-alone. The grid tied battery less are the most popular inverters today. These inverters connect directly to the public utility, using the utility power as a storage battery. The grid-tied with battery backup are more complex than battery less grid-tied inverters because they need to sell power to the grid, supply power to backed-up loads during outages, and charge batteries from the grid, PV or wind turbine after an outage. The stand alone inverters are designed for independent utility-free power system and are appropriated for remote hybrid system installation [Patel, 2006].

In the other hand, based on their output waveforms there are three kinds of inverters; square wave, modified sine-wave, and pure sine wave inverters. Of the three, the square wave type is the simplest and least expensive, but with the poorest quality output signal. The modified sine wave type is suitable for many load types and is the most popular low-cost inverter. Pure sine-wave inverters produce the highest quality signal and are used for sensitive devices such as medical equipment, laser printers, stereos, etc.

The efficiency of converting the direct current to alternative current of most inverters today is 90 percent or more [Rivera, 2008]. Many inverters claim to have higher efficiencies but for this thesis the efficiency that was used is 90%.

CHAPTER 5

HYBRID POWER GENERATION SYSTEM

A hybrid system is a combination of one or more resources of renewable energy such as solar, wind, micro/mini-hydropower and biomass with other technologies such as batteries and diesel generator. As an off-grid power generation, the hybrid system offers clean and efficient power that will in many cases be more cost-effective than sole diesel systems. As a result, renewable energy options have increasingly become the preferred solution for off-grid power generation [Ali B. et al, 2010].

The hybrid system studied in this thesis is one combining solar PV and wind turbine with diesel generator(s) and bank of batteries, which are included for backup purposes. Power conditioning units, such as inverters, are also part of the supply system. Hybrid wind turbine and PV modules, offer greater reliability than any one of them alone because the energy supply does not depend entirely on any one source. For example, on a cloudy stormy day when PV generation is low there's likely enough wind energy available to make up for the loss in solar electricity, and as a result the size of the battery storage can be reduced [Patel, 2006].

Wind and solar hybrids also permit use of smaller, less costly components than would otherwise be needed if the system depends on only one power source. This can substantially lower the cost of a remote power system. In a hybrid system the designer doesn't need to weigh the components for worst-case conditions by specifying a larger wind turbine and battery bank than is necessary [Patel, 2006].

Other advantages of the hybrid system are the stability and immobility of the system and a lower maintenance requirement, thus reducing downtime during repairs or routine maintenance. In addition to this, as well as being indigenous and free, renewable energy resources also contribute to the reduction of emissions and pollution [Getachew, 2009].

The PV-wind hybrid power generation system makes use of the solar PV and wind turbine to produce electricity as the primary source to supply the load. The configuration of PV-wind hybrid system is analyzed for various PV array and wind turbine sizes with respect to a diesel generator to operate in tandem with the battery system. The power conditioning units will determine the ac conversion of the dc power in relation to optimum diesel generator operation following the load profile. The charge controller will charge the batteries with energy from PV modules and wind turbines as well as from the diesel generator. The main objective of PV-wind hybrid system is to reduce the cost of operation and maintenance and cost of logistic by minimizing diesel runtime and fuel consumption. To achieve this generator only runs as needed to recharge the battery and to supply excess load when renewable sources are not enough to supply the load. A schematic of a typical PV-wind hybrid system can be shown in Figure 5.1.

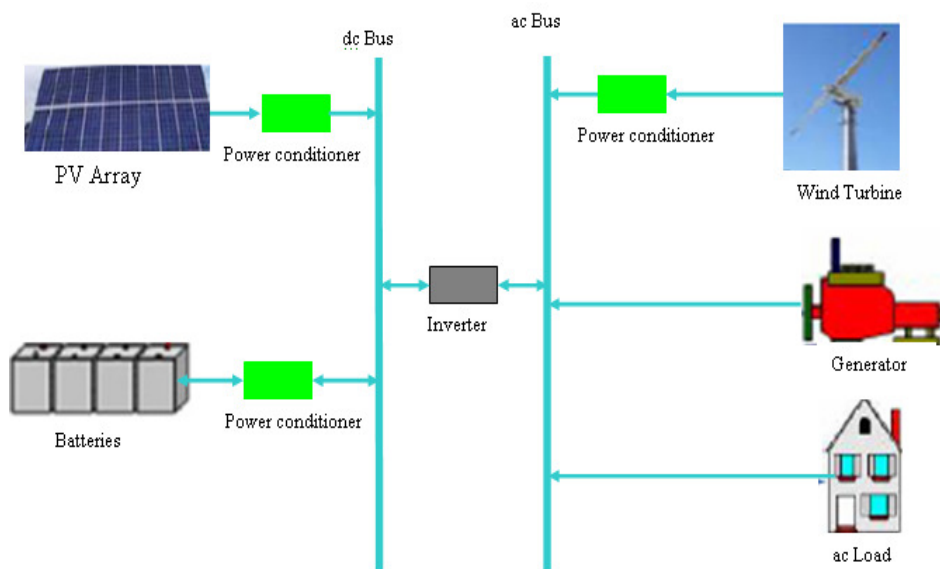


Figure 5.1: General schemes for the standalone hybrid power supply system

The main components of the hybrid system are the wind turbine and the PV panel. Diesel generator(s), a battery bank, and an inverter module are auxiliary parts of the system. The basic principles of these components were covered in the previous chapters.

5.1. Designing and Modeling of Hybrid System with HOMER

The Hybrid Optimization Model for Electric Renewables (HOMER), which is copyrighted by Midwest Research Institute (MRI) is a computer model developed by the U.S. National Renewable Energy Laboratory (NREL) to assist the design of power systems and facilitate the comparison of power generation technologies across a wide range of applications [HOMER, ver. 2.67 Beta]. HOMER is used to model a power system physical behavior and its life-cycle cost, which is the total cost of installing and operating the system over its life time. HOMER allows the modeler to compare many different design options based on their technical and economic merits. It also assists in understanding and quantifying the effects of uncertainty or changes in the inputs.

The design of a stand-alone PV-wind hybrid power supply system to a model community of 100 households, with average six members per family was carried out based on the theoretical background discussed so far. HOMER software is used as a tool to accomplish the research. As mentioned earlier, the main objective of the study is to design and model hybrid PV–Wind–diesel–battery based standalone power generation systems to meet the load requirements of the community specified earlier.

A schematic diagram of the standalone hybrid power supply system required is shown in figure 5.1 and its representation by HOMER is shown in figure 5.2. The power conditioning units are dc-dc and ac-dc converters, with the sole purpose of matching the PV, batteries and wind turbine voltages to that of the bus voltage at the dc bus. The ac load is of both primary and deferrable types. The primary load is an electric demand that must be served according to a particular schedule, whereas deferrable load is electric demand that can be served at certain period of time, the exact timing is not important.

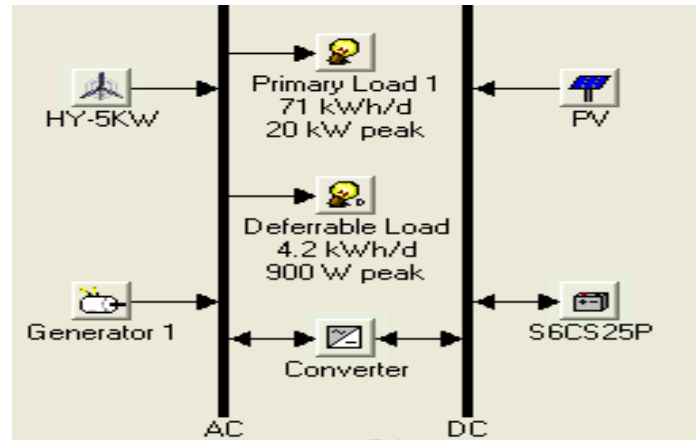


Figure 5.2: HOMER diagram for the hybrid system

HOMER performs three principal tasks: simulation, optimization, and sensitivity analysis based on the raw input data given by user. In the simulation process, the performance of a particular power system configuration for each hour of the year is modeled to determine its technical feasibility and life-cycle cost. In the optimization process, many different system configurations are simulated in search of the one that satisfies the technical constraints at the lowest life-cycle cost. In the sensitivity analysis process, multiple optimizations are performed under a range of input assumptions to judge the effects of uncertainty or changes in the model inputs. Optimization determines the optimal value of the variables over which the system designer has control such as the mix of components that make up the system and the size or quantity of each. Sensitivity analysis helps assess the effects of uncertainty or changes in the variables over which the designer has no control, such as the average wind speed or the future fuel price.

5.1.1. Simulation

The simulation process determines how a particular system configuration, a combination of system components of specific sizes, and an operating strategy that defines how those components work together, would behave in a given setting over a long period of time.

HOMER can simulate a wide variety of micropower system configurations, comprising any combination of a PV array, one or two wind turbines, a run-of-river hydro-turbine, and up to three generators, a battery bank, a dc-ac converter, an electrolyzer, and a hydrogen storage tank. The system can be grid-connected or autonomous and can serve ac and dc electric loads and a thermal load.

Systems that contain a battery bank and one or more generators require a dispatch strategy, which is a set of rules governing how the system charges the battery bank. Dispatch strategy is thoroughly discussed in section 5.1.4.

The simulation process serves two purposes. First, it determines whether the system is feasible. The feasible system is one which can adequately serve the electric and thermal loads and satisfy any other constraints imposed by the user. Second, it estimates the life-cycle cost of the system, which is the total cost of installing and operating the system over its lifetime. The life-cycle cost is a convenient metric for comparing the economics of various system configurations.

A particular system configuration is modeled by performing an hourly time series simulation of its operation over one year. Simulation steps through the year one hour at a time, calculating the available renewable power, comparing it to the electric load, and deciding what to do with surplus renewable power in times of excess, or how best to generate additional power in times of deficit. When one year's worth of calculations is completed, it is determined whether the system satisfies the constraints imposed by the user on such quantities as the fraction of the total electrical demand served, the proportion of power generated by renewable sources, or the emissions of certain pollutants, etc. The quantities required to calculate the system's life-cycle cost, such as the annual fuel consumption, annual generator operating hours, expected battery life are also computed.

The quantity used to represent the life-cycle cost of the system is the total net present cost (NPC). This single value includes all costs and revenues that occur within the project lifetime, with future cash flows discounted to the present. The total net present cost includes the initial

capital cost of the system components, the cost of any component replacements that occur within the project lifetime, the cost of maintenance and fuel.

5.1.2. Optimization

The simulation process models a particular system configuration, whereas the optimization process determines the best possible system configuration. The best possible, or optimal, system configuration is the one that satisfies the user-specified constraints at the lowest total net present cost. Finding the optimal system configuration may involve deciding on the mix of components that the system should contain, the size or quantity of each component, and the dispatch strategy the system should use. In the optimization process, many different system configurations are simulated; the infeasible ones are discarded, the feasible ones are ranked according to total net present cost, and the feasible one is presented with the lowest total net present cost as the optimal system configuration.

The goal of the optimization process is to determine the optimal value of each decision variable that interests the modeler. A decision variable is a variable over which the system designer has control and for which multiple possible values can be considered in the optimization process. Possible decision variables include:

- The size of the PV array
- The number of wind turbines
- The size of each generator
- The number of batteries
- The size of the dc-ac converter
- The dispatch strategy

Optimization can help the modeler find the optimal system configuration out of many possibilities. Multiple values for each decision variable can be entered in search space, which is the table that contains the set of all possible system configurations over which HOMER can search for optimal system configuration. In the optimization process, every system

configuration in the search space is simulated and the feasible ones are displayed in a table, sorted by total net present cost.

5.1.3. Sensitivity Analysis

In the sensitivity analysis process multiple optimizations are performed, each using a different set of input assumptions. A sensitivity analysis reveals how sensitive the outputs are to changes in the inputs.

In a sensitivity analysis, a range of values for a single input variable are fed to HOMER. A variable for which the user has entered multiple values is called a sensitivity variable. Almost every numerical input variable that is not a decision variable can be a sensitivity variable. Examples include the PV module price, the fuel price, the interest rate, etc.

A sensitivity analysis can be performed with any number of sensitivity variables. Each combination of sensitivity variable values defines a distinct sensitivity case. A separate optimization process for each sensitivity case is performed and the results are presented in various tabular and graphic formats.

One of the primary uses of sensitivity analysis is in dealing with uncertainty. If a system designer is unsure of the value of a particular variable, he/she can enter several values covering the likely range and see how the results vary across that range. But sensitivity analysis has applications beyond coping with uncertainty. A system designer can use also sensitivity analysis to evaluate trade-offs between different options.

5.1.4. Hybrid System Modeling

In this section how HOMER models the physical operation of a system is provided in greater detail. A power system must comprise at least one source of electrical or thermal energy (such as a wind turbine, a diesel generator, or the grid), and at least one destination for that energy (electrical or thermal load). It may also comprise conversion devices such as a dc-ac converter

or an electrolyzer, and energy storage devices such as a battery bank or a hydrogen storage tank.

The following subsections devoted to how to model the loads that the system must serve, the components of the system and their associated resources, and how that collection of components operates together to serve the loads.

5.1.4.1. Electric Loads

The electric loads are usually the largest single influence on the size and cost of hybrid system components. So, deciding on the loads is one of the most important steps in the design of the hybrid system.

The term loads refers to a demand for electric or thermal energy, if any. Three types of loads can be modeled using HOMER: primary load which is electric demand that must be served according to a particular schedule, deferrable load which is electric demand that can be served at certain period of time, the exact timing is not important and thermal load which is demand for heat.

Primary Load: Primary load is electrical demand that the power system must meet at a specific time. Electrical demand associated with lights, radio, TV, household appliances, computers, and industrial processes is typically modeled as primary load. If electrical demand exceeds supply, there is a deficit that is recorded as unmet load.

The user specifies an amount of primary load in kW for each hour of the year, either by importing a file containing hourly data or by allowing HOMER to synthesize hourly data from average daily load profiles. When synthesizing load data, HOMER creates hourly load values based on user-specified daily load profiles. Different profiles for different months and different profiles for weekdays and weekends are specified. A specified amount of randomness can be added to synthesize load data so that every day's load pattern is unique. In this thesis 5% hourly and daily load noise is defined to account for variability of load demand.

Among the three types of loads, primary load receives special treatment in that it requires a user-specified amount of operating reserve [HOMER, ver. 2.67 Beta]. Section 5.1.4.4 covers operating reserve in greater detail.

Deferrable Load: Deferrable load is electrical demand that can be met anytime within a certain time span, which exact timing is not important. Water pumping and battery-charging are examples of deferrable loads because the storage inherent to each of those loads allows some flexibility as to when the system can serve them. The ability to defer serving a load is often advantageous for systems comprising intermittent renewable power sources, because it reduces the need for precise control of the timing of power production. If the renewable power supply ever exceeds the primary load, the surplus can serve the deferrable load rather than going to waste.

For each month, the user specifies the average deferrable load, which is the rate at which energy drains out of the tank. The user also specifies the storage capacity in kWh (the size of the tank), and the maximum and minimum rate at which the power system can put energy into the tank.

According to Getachew, electric load in the rural villages of Ethiopia can be assumed to be composed of lighting, radio receiver and television set, water pumps, health post and primary schools load [Getachew, 2009]. Bimrew considered only lighting, radio and television as a community load [Bimrew, 2007]. In this study, electricity for flour mills is added to the load together with radio receiver and health post is upgraded to health clinic with additional medical equipment. Water pumps are considered as deferrable loads while the others as primary loads. As introduced earlier, the community understudy, which equipped with school and a health clinic, has 100 households with an average 6 members per family.

The electric loads for school and community contains lighting, water pumping, a radio receiver and flour mills. Whereas health clinic loads includes lighting, water pumping, electric supply necessary for some medical equipment, and other for miscellaneous use.

In the calculation of the load or, in general, the design of hybrid system includes those components which are locally available without considering their efficiencies. This is done for both load and power generation sides.

Water pumping systems, deferrable load, is required for the households, the school and health clinic. A minimum of 100 liters of water per day per family and 2000 l/day for health clinic and primary school each is suggested. To accomplish this, 4 pumps of 150 W (with a capacity of 10 l/m) operating for 6 hours/day are to be installed to supply water for the community. Another 2 pumps of 150W (with a capacity of 10 l/m) for the school and health clinic each operating for 4 hours/day is assumed. A sufficient water storage capacity for 3 days is assumed and the corresponding electricity storage capacity is 10.8 kWh for the households and 5.4 kWh for the school and health clinic. The peak deferrable load (rated power of the pumps) is 0.6 kW for the households and 0.3 kW for the school and health clinic.

Each household is assumed to use a 7 W for night external lighting, a 3 W radio receiver and two 40 W light bulbs to be used between 18:00 to 23:00 in the evening and the daily energy consumption is calculated to be approximately 46 kWh.

Electric lighting for the school in the evenings (18:00-21:00) for those who wish to pursue basic education is suggested. For eight classrooms with eight lamps of 40 watt capacity in each classroom and a lamp for a toilet and eight fans for each class is considered for air conditioning which operate for eight hours and energy is calculated to 4.6 kWh/day.

A typical health clinic, equipped with vaccine refrigerator, light bulbs, stand-by communication VHF radio, microscope, vaporizer, centrifugal nebulizer, oxygen concentrator, fans and AM/FM radio receiver, is suggested. The health clinic has ten bed rooms, one reception room, two OPD rooms and other rooms for different services. This equipment of a health clinic consumes 22.4kWh/day.

The sum total of the daily energy consumption of the community is approximately 78 kWh.

In the weekends it is assumed that flour mills are not working and evening classes are conducted at day time. In the rainy season up to 30% deferrable load can be expected to decrease because water consumption from the pumps is expected to be shared by river and rain water ponds [Getachew, 2009]. September to October and April to June is the rainy season for this area. There are no classes in July and August (annual break) and in January (semester break). The daily electrical energy consumption in the rainy months would be 76 kWh and that in January, July and August 73 kWh. Thus the yearly electrical energy consumption pattern is that given in Table 5.1.

Table 5.1: Monthly average daily electrical energy consumption (kWh)

Months	Jan	Feb-Mar	Apr-June	Jul-Aug	Sep-Oct	Nov-Dec
Deferrable Load	4.5	5.4	3.8	4.5	3.8	5.4
Primary Load	68.5	72.6	72.2	68.5	72.2	72.6
Total Load	73	78	76	73	76	78

The 24 hour primary and deferrable load profiles are given in figures 5.3 and 5.4 respectively.

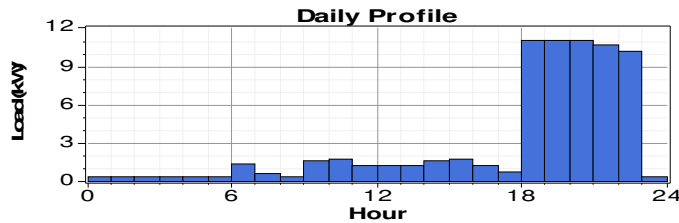


Figure 5.3: Primary load profile of the community

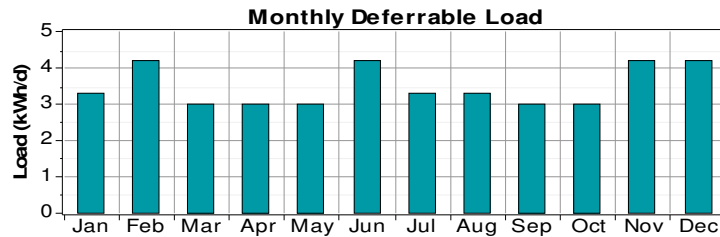


Figure 5.4: Monthly average deferrable load profiles

5.1.4.2. Resources

The term resource applies to anything coming from outside the system that is used by the system to generate electric or thermal power. That includes the four renewable resources (solar, wind, hydro, and biomass) as well as any fuel used by the components of the system. Renewable resources depend extremely on location. The solar resource depends strongly on latitude and climate, the wind resource on large-scale atmospheric circulation patterns and geographic influences, the hydro resource on local rainfall patterns and topography, and the biomass resource on local biological productivity. Moreover, at any one location a renewable resource may exhibit strong seasonal and hour-to-hour variability. The nature of the available renewable resources affects the behavior and economics of renewable power systems, since the resource determines the quantity and the timing of renewable power production. The careful modeling of the renewable resources is therefore an essential element of system modeling. In this section how to model the renewable resources used in this thesis and the fuel is described.

Solar Resource: To model a system containing a PV array, the solar resource data for the location of interest has been provided. Solar resource data indicate the amount of global solar radiation (beam radiation coming directly from the sun, plus diffuse radiation coming from all parts of the sky) that strikes Earth's surface in a typical year. The data can be in one of three forms: hourly average global solar radiation on the horizontal surface (kW/m^2), monthly average global solar radiation on the horizontal surface ($\text{kWh/m}^2\cdot\text{day}$), or monthly average clearness index. The clearness index is the ratio of the solar radiation striking Earth's surface to the solar radiation striking the top of the atmosphere. A number between zero and one, the clearness index is a measure of the clearness of the atmosphere.

HOMER generates synthetic hourly global solar radiation data from monthly solar resource data using the Graham algorithm [HOMER, ver. 2.67 Beta]. The inputs to this algorithm are the monthly average solar radiation values and the latitude. The output is an 8760-hour data set with statistical characteristics similar to those of real measured data sets.

Wind Resource: To model a system comprising one or more wind turbines, the wind resource data indicating the wind speeds the turbines would experience in a typical year has been provided. The user can provide measured hourly wind speed data if available. Otherwise,

HOMER can generate synthetic hourly data from 12 monthly average wind speeds and four additional statistical parameters: the Weibull shape factor, the autocorrelation factor, the diurnal pattern strength, and the hour of peak wind speed.

The Weibull shape factor is a measure of the distribution of wind speeds over the year (see section 2.4). The autocorrelation factor is a measure of how strongly the wind speed in one hour tends to depend on the wind speed in the preceding hour [HOMER, ver. 2.67 Beta]. For complex topography the autocorrelation factor is (0.70 - 0.80) while for a uniform topography the range is higher, (0.90 - 0.97). A typical range for the autocorrelation factor is 0.8 – 0.95 [HOMER, ver. 2.67 Beta]. An average value of 0.85 is used here because the selected areas are of averagely uniform topography. The diurnal pattern strength is a measure of how strongly the wind speed tends to depend on the time of day [HOMER, ver. 2.67 Beta]. Typical values for diurnal pattern strength range from 0 to 0.4. A value of 0.25 has been selected for calculations. The hour of peak wind speed is the hour of the day that tends, on average, to be the windiest throughout the year. The typical range for the time of peak wind speed is 14:00-16:00 [HOMER ver. 2.67 Beta]. This has also been observed in the available raw data for some of the months. In addition to this, the software has been run for different times between 14:00 and 18:00, the results have been checked against the measured data and the time of 15:00 has been chosen for the calculations.

The anemometer height, which is the height above ground at which the wind speed data were measured, has been defined. The elevation of the site above sea level, which is used to calculate the air density according to equations 2.10-2.12, is also defined.

Fuel: HOMER provides a library of several predefined fuels, and users can add to the library if necessary. The physical properties of a fuel include its density, lower heating value, carbon content, and sulfur content. The user can also choose the most appropriate measurement units, L, m³, or kg. The two remaining properties of the fuel are the price and the annual consumption limit.

5.1.4.3. Components

A component is any part of a power system that either generates, delivers, converts, or stores energy. HOMER models 10 types of components. Three of components generate electricity from intermittent renewable sources: photovoltaic modules, wind turbines, and hydro turbines. Another two types of components, generators and the grid are dispatchable energy sources, meaning that the system can control them as needed. Two types of components, converters and electrolyzers, convert electrical energy into another form. Converters convert electricity from ac to dc or from dc to ac. Electrolyzers convert surplus ac or dc electricity into hydrogen via the electrolysis of water. Other component a reformer generates hydrogen by reforming a hydrocarbon, typically natural gas. The system can store the hydrogen produced by electrolyzer and reformer and use it as fuel for one or more generators. Finally, two types of components store energy: batteries and hydrogen storage tanks.

Cost minimization is the primary criterion considered when selecting the components.

In this section how to model the components used in this thesis and discuss the physical and economic properties that the user can use to describe each is explained.

PV Array: The PV array is a device that produces dc electricity in direct proportion to the global solar radiation incident upon it. The power output of the PV array is calculated using the following equation [HOMER, ver. 2.67 Beta]:

$$P_{PV} = Y_{PV} f_{PV} \left(\frac{\bar{G}_T}{\bar{G}_{T,STC}} \right) \left[1 + \alpha_p (T_c - T_{c,STC}) \right] \quad 5.1$$

where Y_{PV} is the rated capacity of PV array (kW), f_{PV} is the PV derating factor (%), \bar{G}_T is the solar radiation incident on the PV array in the current time step (kW/m²), $\bar{G}_{T,STC}$ is the incident radiation at standard test conditions (1 kW/m²), α_p is the temperature coefficient of power (%/°C), T_c is the PV cell temperature in the current time step (°C), and $T_{c,STC}$ is the PV cell temperature under standard test conditions (25 °C)

If the effect of temperature on the PV array is not considered, the above equation simplifies to:

$$P_{PV} = Y_{PV} f_{PV} \left(\frac{\overline{G}_T}{\overline{G}_{T,STC}} \right) \quad 5.2$$

The rated capacity (sometimes called the peak capacity) of a PV array is the amount of power it would produce under standard test conditions of 1 kW/m² irradiance and a panel temperature of 25°C.

The derating factor is a scaling factor meant to account for effects of dust on the panel, wire losses, elevated temperature, or anything else that would cause the output of the PV array to deviate from that expected under ideal conditions.

To describe the cost of the PV array, its initial capital cost in dollars, replacement cost in dollars, and operating and maintenance (O&M) cost in dollars per year has been specified. The replacement cost is the cost of replacing the PV array at the end of its useful lifetime, which is specified in years. By default, the replacement cost is equal to the capital cost, but the two can differ for several reasons. For example the user may want to account for a reduction over time in the purchase cost of a particular technology. In this thesis replacement cost is taken as 70% of initial capital cost taking into account the reduction of PV cost trends.

Wind Turbine: A wind turbine is a device that converts the kinetic energy of the wind into ac or dc electricity according to a particular power curve, which is a graph of power output versus wind speed at hub height.

Each hour, the power output of the wind turbine is calculated in a four-step process. First, the average wind speed for the hour at the anemometer height is determined by referring to the wind resource data. Second, the corresponding wind speed at the turbine's hub height is calculated using either the logarithmic law or power law. Third, the power output of wind turbine is calculated at that wind speed referring to its power curve assuming standard air

density. Fourth, that power output value is multiplied by the air density ratio, which is the ratio of the actual air density to the standard air density.

In addition to the turbine's power curve and hub height, the expected lifetime of the turbine in years, its initial capital cost in dollars, its replacement cost in dollars, and its annual O&M cost in dollars per year has been specified.

The primary criterion for the selection of the wind turbine is its cost. The wind turbines have been selected from different sources; the various wind turbine websites and those suggested by the HOMER program itself based on their costs. Other selection criteria used are: the type of current they generate (ac or dc), how low the cut-in wind speed is, and for what application the wind turbine be used for. The cut-in wind speed is another primary criterion, if not import than cost, as the wind resource at the site is not very high. The type of current they generate, whether ac or dc, is also considered as it have impacts on the size of the inverter. As the load assumed for the households is of an ac type a wind turbine that generates ac current has been chosen. As the aim of the research is to supply electric energy to remotely located communities, the wind turbines selected should be those which are applicable for home or off-grid applications.

Based on the selection criteria mentioned above, different wind turbines have been tested by running the simulation several times. From those wind turbines which were candidates for this application, the HY-5 type has been found to be the best in terms of the cut-in wind speed and also in respect to other criteria mentioned earlier. This wind turbine was obtained from those wind turbine website (www.huayingwindpower.com) owned by Hulk Energy Machinery. The turbine is a 5 kW turbine commonly available on the market such as the one for which the power curve is given in figure 2.4.

Generators: A generator consumes fuel to produce electricity, and possibly heat as a by-product. The generator module is flexible enough to model a wide variety of generators, including internal combustion engine generators, micro-turbines, fuel cells, etc.

The principal physical properties of the generator are its maximum and minimum electrical power output, its expected lifetime in operating hours, the type of fuel it consumes, and its fuel curve, which relates the quantity of fuel consumed to the electrical power produced.

The fuel curve is a straight line with a y-intercept and uses the following equation for the generator's fuel consumption [HOMER, ver. 2.67 Beta]:

$$F = F_0 Y_{gen} + F_1 P_{gen} \quad 5.3$$

where: F is fuel consumption in this hour (L), F_0 is generator fuel curve intercept coefficient (L/hr/kW_{rated}), F_1 is generator fuel curve slope (L/hr/kW), Y_{gen} is rated capacity of generator (kW), and P_{gen} is output of the generator in this hour (kW).

In addition to these properties, the generator emissions coefficients, which specify the generator's emissions of six different pollutants in grams of pollutant emitted per quantity of fuel consumed can be specified.

The generator's initial capital cost in dollars, replacement cost in dollars, and annual O&M cost in dollars per operating hour has been specified. The generator O&M cost should account for oil changes and other maintenance costs, but not fuel cost because fuel cost is calculated separately. Fixed and marginal cost of energy has been calculated for each dispatchable power source. The fixed cost of energy is the cost per hour of simply running the generator, without producing any electricity. The marginal cost of energy is the additional cost per kWh of producing electricity from that generator.

The following equation is used to calculate the generator's fixed cost of energy [HOMER, ver. 2.67 Beta]:

$$c_{gen, fixed} = c_{om, gen} + \frac{C_{rep, gen}}{R_{gen}} + F_0 Y_{gen} c_{fuel, eff} \quad 5.4$$

where: $c_{om,gen}$ is the O& M cost (\$/hr), $C_{rep,gen}$ is the replacement cost (\$), R_{gen} is the generator lifetime (hr), F_0 is generator fuel curve intercept coefficient (L/hr/kW_{rated}), Y_{gen} is rated capacity of generator (kW), and $c_{fuel,eff}$ is the effective price of fuel (\$/L). The effective price of fuel includes the cost penalties, if any, associated with the emissions of pollutants from the generator.

The marginal cost of energy of the generator is calculated using the following equation:

$$c_{gen,mar} = F_1 c_{fuel,eff} \quad 5.5$$

where: F_1 is generator fuel curve slope (L/hr/kW), and $c_{fuel,eff}$ is the effective price of fuel (\$/L).

Battery Bank: The battery bank is a collection of one or more individual batteries. A battery is a device capable of storing a certain amount of DC electricity at a fixed round-trip energy efficiency, with limits as to how quickly it can be charged or discharged, how deeply it can be discharged without causing damage, and how much energy can cycle through it before it needs replacement.

The key physical properties of the battery are its nominal voltage, capacity curve, lifetime curve, minimum state of charge, and round-trip efficiency. The capacity curve shows the discharge capacity of the battery in ampere-hours versus the discharge current in amperes. Manufacturers determine each point on this curve by measuring the ampere-hours that can be discharged at a constant current out of a fully charged battery. Capacity typically decreases with increasing discharge current. The lifetime curve shows the number of discharge-charge cycles the battery can withstand versus the cycle depth. The number of cycles to failure typically decreases with increasing cycle depth. The minimum state of charge is the state of charge below which the battery must not be discharged to avoid permanent damage. The round-trip efficiency indicates the percentage of the energy going into the battery that can be drawn back out.

To calculate the battery's maximum allowable rate of charge or discharge, the kinetic battery model is used, which treats the battery as a two-tank system [HOMER, ver. 2.67 Beta].

Three parameters describe the battery: The maximum capacity of the battery which is the combined size of the available and bound tanks; the capacity ratio which is the ratio of the size of the available tank to the combined size of the two tanks and the rate constant which is analogous to the size of the pipe between the tanks.

It is assumed that lifetime throughput is independent of cycle depth and estimate the life of the battery bank simply by monitoring the amount of energy cycling through it, without having to consider the depth of the various charge–discharge cycles. The life of the battery bank in years is found as follows [HOMER, ver. 2.67 Beta]:

$$R_{batt} = MIN \left(\frac{N_{batt} \cdot Q_{lifetime}}{Q_{thrpt}}, R_{batt,f} \right) \quad 5.6$$

where: R_{batt} is battery bank life (yr), N_{batt} is number of batteries in the battery bank, $Q_{lifetime}$ is lifetime throughput of a single battery (kWh), Q_{thrpt} is annual battery throughput (the total amount of energy that cycles through the battery bank in one year) (kWh/yr), and $R_{batt,f}$ is battery float life (the maximum life regardless of throughput) (yr)

The battery bank's capital and replacement costs in dollars, and the O&M cost in dollars per year have been specified. Since the battery bank is a dispatchable power source, its fixed and marginal cost of energy is calculated for comparison with other dispatchable sources. Unlike the generator, there is no cost associated with “operating” the battery bank so that it is ready to produce energy; hence its fixed cost of energy is zero. For its marginal cost of energy, the sum of the battery wear cost (the cost per kWh of cycling energy through the battery bank) and the battery energy cost (the average cost of the energy stored in the battery bank) are used. The battery wear cost is calculated as [HOMER, ver. 2.67 Beta]:

$$c_{bw} = \frac{C_{rep,batt}}{N_{batt} \cdot Q_{lifetime} \cdot \sqrt{\eta_{rt}}} \quad 5.7$$

where: $C_{rep,batt}$ is replacement cost of the battery bank (\$) and η_{rt} is battery roundtrip efficiency (%)

Converter: A converter is a device that converts electric power from dc to ac in a process called inversion, and/or from ac to dc in a process called rectification. The converter size, which is a decision variable, refers to the inverter capacity, meaning the maximum amount of ac power that the device can produce by inverting dc power. The rectifier capacity, which is the maximum amount of dc power that the device can produce by rectifying ac power, as a percentage of the inverter capacity has been specified.

The final physical properties of the converter are its inversion and rectification efficiencies, which are assumed to be constant. The economic properties of the converter are its capital and replacement cost in dollars, its annual O&M cost in dollars per year, and its expected lifetime in years.

5.1.4.4. Dispatch Strategy

In addition to modeling the behavior of each individual component, how those components work together as a system has been simulated. That requires hour-by-hour decisions as to which generators should operate and at what power level, whether to charge or discharge the batteries. In this section the logic used to make such decisions is described briefly. A discussion of operating reserve comes first because the concept of operating reserve significantly affects dispatch decisions.

Operating Reserve: Operating reserve provides a safety margin that helps ensure reliable electricity supply despite variability in the electric load and the renewable power supply. Virtually every real power system must always provide some amount of operating reserve,

because otherwise the electric load would sometimes fluctuate above the operating capacity of the system, and an outage would result.

At any given moment, the amount of operating reserve that a power system provides is equal to the operating capacity minus the electrical load. The required amount of operating reserve has been specified, and HOMER simulates the system so as to provide at least that much operating reserve.

Each hour, the required amount of operating reserve is calculated as a fraction of the primary load of that hour, plus a fraction of the annual peak primary load, plus a fraction of the PV power output of that hour, plus a fraction of the wind power output of that hour. In this study an operating reserve of 10, 25 and 50 % of the hourly load, solar power output and wind power output respectively is used.

It is assumed that both dispatchable and nondispatchable power sources provide operating capacity. A dispatchable power source provides operating capacity in an amount equal to the maximum amount of power it could produce at a moment's notice. For a generator, that is equal to its rated capacity if it is operating or zero if it is not operating. For the battery, that is equal to its current maximum discharge power, which depends on state of charge and recent charge-discharge history. In contrast to the dispatchable power sources, the operating capacity of a nondispatchable power source (a PV array or wind turbine) is equal to the amount of power the source is currently producing, as opposed to the maximum amount of power it could produce.

If a system is ever unable to supply the required amount of load plus operating reserve, the shortfall is recorded as capacity shortage. The maximum allowable capacity shortage fraction is specified. Any system whose capacity shortage fraction exceeds this constraint is discarded as infeasible. In this thesis the capacity shortage is not tolerable i.e. zero fraction of capacity shortage is defined.

Control of Dispatch-able System Components: Each hour of the year, it is determined whether the renewable power sources by themselves are capable of supplying the electric load and the required operating reserve. If not, how best to dispatch the dispatchable system components (the generators and battery bank) to serve the loads and operating reserve is determined. This determination of how to dispatch the system components each hour is the most complex part of simulation logic.

The fundamental principle that is followed when dispatching the system is the minimization of cost. The economics of each dispatchable energy source is represented by two values: a fixed cost in dollars per hour, and a marginal cost of energy in dollars per kWh. These values represent all costs associated with producing energy with that power source that hour. Using these cost values, the combination of dispatchable sources that can serve the electrical load and the required operating reserve at the lowest cost is searched. Satisfying the loads and operating reserve without any capacity shortage is paramount. But among the combinations of dispatchable sources that can serve the loads equally well, the one that does so at the lowest cost is chosen.

Dispatch Strategy: The economic dispatch logic described in the previous section governs the production of energy to serve loads and hence applies to all systems. But for systems comprising both a battery bank and a generator, an additional aspect of system operation arises, which is how the generator should charge the battery bank. This battery-charging logic cannot be based on simple economic principles, because there is no deterministic way to calculate the value of charging the battery bank.

HOMER provides two simple strategies and lets the user model them both to see which is better in any particular situation. These dispatch strategies are called load-following and cycle-charging. Under the load-following strategy, a generator produces only enough power to serve the load, and does not charge the battery bank. Under the cycle-charging strategy, whenever a generator operates, it runs at its maximum rated capacity and charges the battery bank with the excess. Both cycle-charging (CC) and load-following (LF) dispatch strategies are analyzed to determine which is optimal in a given situation.

Additional information input into HOMER is summarized in Table 5.2. The values given in this table are primarily chosen according to the size of the load for the assumed hypothetical community. The monthly average daily electrical energy consumption is given in Table 5.1. This energy consumption, in kWh/day, varies between 73kWh/day and 78 kWh/day from month to month. In terms of variation of power on a daily basis, this is given in figure 5.3 for the primary load and figure 5.4 shows the community's deferrable load power demand on a monthly basis. These are the principal guidelines for selecting the size of the power components listed in Table 5.2. As mentioned previously the components are chosen by considering the local availability of the components without giving attention to their efficiencies.

The costs are estimated according to the current local and global price of the components. Other inputs into the software, such as the range of sizes for the PV, wind turbines and the converter and the number of batteries, are given so as to give flexibility to the software and optimize the output results.

Table 5.2: Inputs to the HOMER software

	PV	Wind Turbine	Diesel Generator	Battery (Surrete 6CS25P)	Converter
Size (kW)	1	5	15	1156Ah	1
Capital (\$)	1200-4500	5000	9000	900	800
O&M cost (\$/yr)	0	100	0.5	20	0
Size considered (kW)	0,5,10,15, 20,25,30,35,40		0,6,10,15,20	_____	0,10,15,20
Quantities considered	_____	0,1, 2, 3	_____	0,1,4,8,12,16, 24, 32	_____
Lifetime	25 yrs	25 yrs	20,000 hrs	9,645 kWh	15yrs

For the analysis, diesel is considered for the generator fuels with prices used are 0.5, 0.8, 0.9, and 1.2 US dollars per liter. The current diesel price considered is 0.9 USD per liter. Inverter

and rectifier efficiencies are assumed as 90%. The project life time is 25 years, and the interest rate is assumed to be the present rate, 6%.

The software generates the results which are a list of feasible power supply systems sorted according to their net present cost. Furthermore, sensitivity variables, such as the range of wind speeds, range of radiation levels, PV panel price, and diesel price are supplied, and then the software is tuned for optimum results.

CHAPTER 6

RESULTS AND CONCLUSIONS

In this chapter the results of the design of a PV-wind hybrid power generation system is presented, the conclusions from the findings are drawn and at the end the recommendations are made. The design of hybrid system, which supplies electricity to model community, was introduced previously. As mentioned in the earlier sections in the design the system components that are locally available have been included without much concern to the efficiency. The results of the investigation will be presented in the following paragraphs.

6.1. Results and Discussions

The monthly average wind speed for Bulbul, together with other related data, such as values of Weibull parameter k , diurnal pattern, autocorrelation, etc, was fed into HOMER. Figure 6.1 shows the wind speed resource data measured at 2 m height.

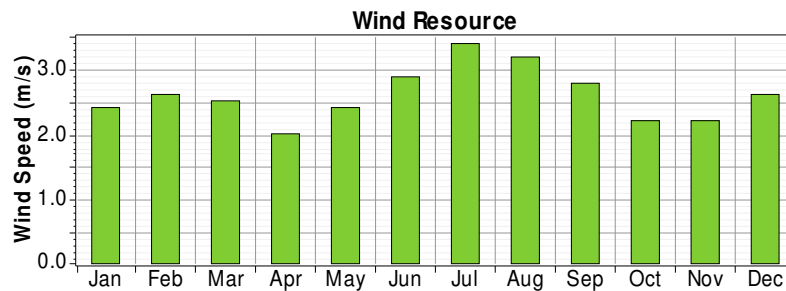


Figure 6.1: Monthly average wind resources

Similarly, the solar energy potential of the site was fed into HOMER and this is depicted in figure 6.2. This figure also shows the clearness index, the ratio of the solar radiation striking Earth's surface to the solar radiation striking the top of the atmosphere, which HOMER generated from global solar radiation for the analysis. Typical values for the monthly average clearness index range from 0.25 (a very cloudy month) to 0.75 (a very sunny month).

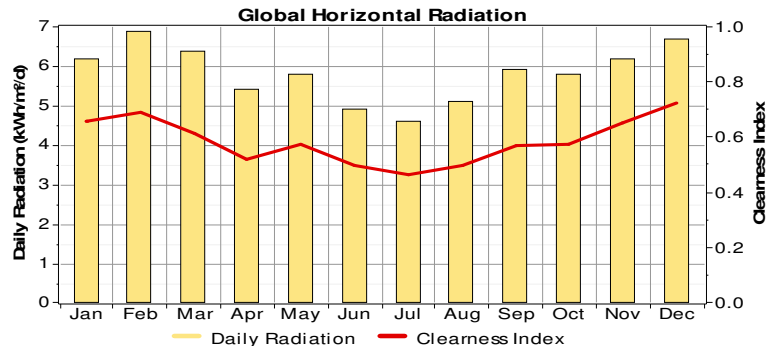


Figure 6.2: Monthly average solar resources

After entering the wind and solar resource data into software, to find the optimum solutions, HOMER is run repeatedly by varying parameters that have a controlling effect over the output. The parameters that have controlling effect on output are given in table 5.2. In addition to those input parameters, multiple prices of diesel oil and PV modules have been used for sensitivity analysis. The output of the simulation is a list of feasible combinations of PV, wind-turbine, generator, converter, and battery hybrid system set-up. The optimization results are generated in either of two forms; an overall form in which the top-ranked system configurations are listed according to their net present cost (NPC) and in a categorized form where only the least-cost system configuration is considered for each system type. Table 6.1 shows a list of the possible combinations of system components in an overall form while table 6.3 represents optimization results in a categorized form. The tables are generated based on a particular set of inputs selected from the input summary table (table 5.2) and the solar and wind resource data for site. The diesel price is 0.9\$/L and the PV capital multiplier is 0.6 (3000 \$/kW). The price of PV has been checked using different sources on the internet and the price ranged from \$1.37 to \$4.6 per watt [EcoBusinessLinks, 2011], [SolarBuzz, 2011], [Solar Panel Price, 2010]. The solar and wind data inputs are the results of investigation of solar and wind potentials of the site; the diesel price is the current price of diesel in the country and the price of PV is also the current price of PV panels in global market obtained from different websites.

The overall form table is too long to fit in this section, so it has been truncated and only a selected part is shown in table 6.1. The complete table is available in the appendix (Table 8.1).

Table 6.1: Overall optimization results

PV (kW)	HY-5	Gen1 (kW)	Battery	Converter (kW)	Dispatch Strategy	Initial Capital	Total NPC	COE (\$/kWh)	RF	Diesel (L)	Gen1 (hrs)
5	3	15	16	15	LF	\$56,937	\$103,914	0.302	0.84	1,955	633
5	3	20	16	15	LF	\$57,952	\$106,553	0.309	0.83	2,173	529
10	3	15	16	15	LF	\$65,937	\$108,489	0.315	0.89	1,655	537
5	2	15	16	15	LF	\$51,947	\$109,014	0.317	0.74	2,703	874
5	3	15	16	20	LF	\$60,937	\$109,213	0.317	0.84	1,951	632
10	2	15	16	15	LF	\$60,947	\$109,325	0.318	0.83	2,129	691
10	3	20	16	15	LF	\$66,952	\$111,272	0.323	0.87	1,865	454
5	3	20	16	20	LF	\$61,952	\$111,569	0.324	0.83	2,148	523
5	2	20	16	15	LF	\$52,962	\$111,649	0.324	0.72	2,965	722
10	2	20	16	15	LF	\$61,962	\$112,311	0.326	0.81	2,390	582
10	3	15	16	20	LF	\$69,937	\$113,580	0.33	0.89	1,636	531
10	2	15	16	20	LF	\$64,947	\$114,514	0.333	0.83	2,118	687
15	2	15	16	15	LF	\$69,947	\$115,728	0.336	0.87	1,959	636
10	3	20	16	20	LF	\$70,952	\$116,116	0.337	0.87	1,828	445
15	3	15	16	15	LF	\$74,937	\$116,144	0.337	0.91	1,562	507
10	2	15	32	15	LF	\$75,347	\$116,780	0.339	0.92	857	278
5	3	15	32	15	LF	\$71,337	\$117,050	0.34	0.91	1,064	345
10	2	20	16	20	LF	\$65,962	\$117,384	0.341	0.81	2,370	577
10	3	15	32	15	LF	\$80,337	\$118,315	0.344	0.96	530	172
10	2	20	32	15	LF	\$76,362	\$118,571	0.344	0.91	961	234
5	3	20	32	15	LF	\$72,352	\$118,808	0.345	0.9	1,175	286
15	3	20	16	15	LF	\$75,952	\$119,073	0.346	0.9	1,778	433
15	2	20	16	15	LF	\$70,962	\$119,084	0.346	0.85	2,230	543
15	1	15	16	15	LF	\$64,957	\$119,800	0.348	0.79	2,639	856
10	2	15	32	20	LF	\$79,347	\$120,081	0.349	0.93	715	231
10	3	15	32	20	LF	\$84,337	\$120,366	0.35	0.98	302	98
15	3	10	32	20	LF	\$92,322	\$125,456	0.364	0.99	84	40
20	3	6	32	20	LF	\$96,730	\$129,593	0.376	1	18	13

The following remarkable results can be noted from the table. The most cost effective system, i.e. the system with the lowest net present cost, is the PV-wind turbine-generator-battery-converter set-up with the generator operating under a load following (LF) strategy (a dispatch strategy whereby the generator operates to produce just enough power to meet the primary load; lower-priority objectives, such as charging the battery bank or serving the deferrable load, is left to the renewable power sources). For this set-up, the total net present cost (NPC) is \$103,914, the cost of energy (COE) is 0.302 \$/kWh, contribution from renewable resources is

84%, the amount of diesel oil used annually is 1,955 liters and the generator operates for 633 hours per year.

In this set-up the part that renewable resources contribute to the supply system is quite significant, being 84%. This setup could be a good choice for implementation. Figure 6.3 shows the monthly average electrical production of this system. Table 6.4 gives some of the main information about the system. The cost breakdown supported by a column-chart for this set-up is also given in figure 6.7.

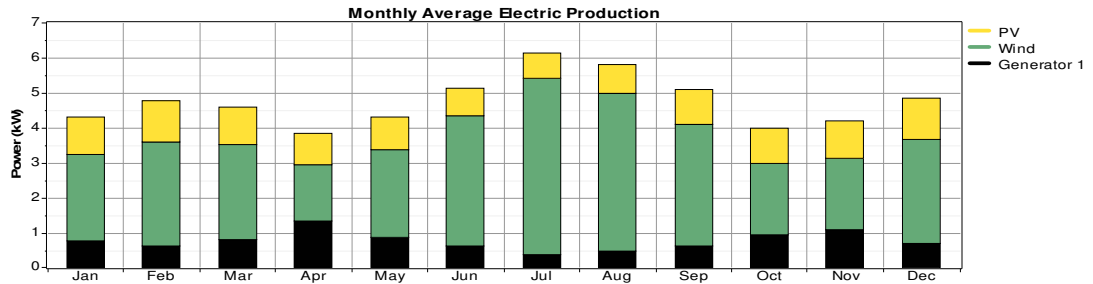


Figure 6.3: Contribution of the power units with 84 % RF, 1st row in Table 6.1

The second most cost effective system is one with NPC \$106,553 and COE 0.309\$/kWh which is the same system type with that of first row. For this setup the part contributed by renewable resources is almost equal with that of first row, being 83%. The monthly average electric production for this setup is shown in Figure 6.4 and Table 6.5 gives the most import information about the system. The cost breakdown supported by a column-chart for this set-up is also given in figure 6.8. Down in the list, there is another system with the same system type with earlier setups having about 96% contribution from renewable resources for a total NPC of \$118,315 and COE of 0.344\$/kWh. This is an increase of about 14 % in the cost over the most cost effective setup but the renewable fraction has increased from 84 % to 96 % making it another good candidate for implementation. The monthly average power production for the 96% renewable fraction set-up in table 6.1 is given in figure 6.5. Key information about the system is also given in table 6.6. The cost breakdown supported by a column-chart is also given in figure 6.9.

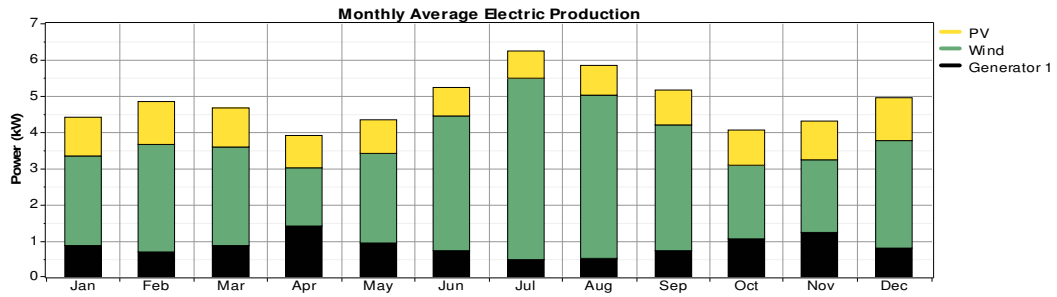


Figure 6.4: Contribution of the power units with 83 % RF, 2nd row in Table 6.1

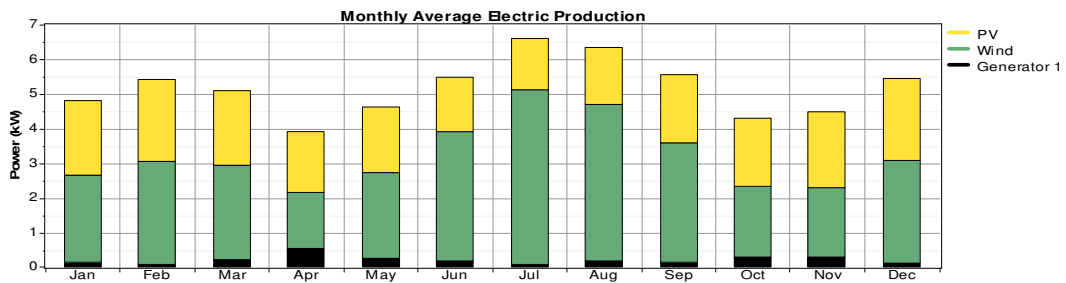


Figure 6.5: Contribution of the power units with 96 % RF

Further down in the list, at bottom of the table, there is another setup with a 100% contribution from renewable resources. For this setup the total NPC increases to \$129,593 and the COE 0.376\$/kWh which is an increase of 10% over the NPC of setup with a 96% renewable resource contribution.

This is another attractive system if the 100% renewable resources contribution is to be given main concern and also if consideration is given to other related issues, such as the future price trend of the components which make up the system, the unpredicted rise in current fossil fuel prices at global market, and also the global warming and environmental protections. The monthly average power production for this configuration is given in figure 6.6. Information

about the system is also given in table 6.7. The cost breakdown supported by a column-chart is also given in figure 6.10.

As mentioned earlier, the price variation for diesel oil, considered in this study, is between \$0.5 and \$1.2. To know what the situation would look like if the current diesel price reached the highest level considered, the first few lines of the optimization results are given in Table 6.2. As can be seen from the table the minimum total NPC in the list is \$117,411, which is about 13% more than the minimum total NPC given in Table 6.1.

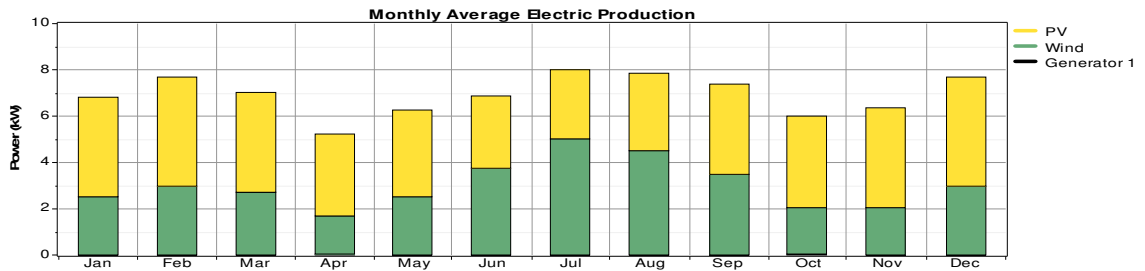


Figure 6.6: Contribution of the power units with 100 % RF, bottom row of Tab. 6.1

Table 6.2: The first few lines of the optimization results for a diesel price of \$1.20

PV (kW)	HY-5	Gen1 (kW)	Battery	Converter (kW)	Dispatch strategy	Initial capital	Total NPC	COE (\$/kWh)	RF	Diesel (L)	Gen1 (hrs)
5	3	15	16	15	LF	\$62,937	\$117,411	0.341	0.84	1,955	633
5	3	20	16	15	LF	\$63,952	\$120,886	0.351	0.83	2,173	529
5	3	15	16	20	LF	\$66,937	\$122,694	0.356	0.84	1,951	632
	3	15	16	15	LF	\$47,937	\$124,465	0.362	0.71	3,118	1,005
5	2	15	16	15	LF	\$57,947	\$125,382	0.364	0.74	2,703	874
5	3	20	16	20	LF	\$67,952	\$125,807	0.365	0.83	2,148	523
	3	15	16	10	LF	\$43,937	\$126,016	0.366	0.69	3,483	1,128

The result in a categorized form, where only the least cost effective system is considered for each system type, is given in table 6.3. The setup in the first row of this table that with an 84 % contribution made by renewable is the same as that listed in Table 6.1 and has been discussed earlier. In this table two system set-ups are of greatest interest, each supplying 100 % from renewable resources. One comprises PV, Wind turbine, Battery, and Converter and the other PV, Battery and Converter. The NPC for the first is \$137,494 and that for the second is \$188,945. The COE are 0.399\$/kWh and 0.549\$/kWh respectively.

The net present costs for these two set-ups are 34% and 82% respectively more than that of the setup with an 84 % renewable contribution listed in first row. However, these set-ups could also be considered as options if issues discussed earlier are given consideration; the issues of future price trends of the components which constitute the system and also the rapidly rising diesel price as well as the issues of environmental protections and global warming.

Table 6.3: optimization results in a Categorized form

PV (kW)	HY-5	Gen1 (kW)	Battery	Converter (kW)	Dispatch strategy	Initial capital	Total NPC	COE (\$/kWh)	RF	Diesel (L)	Gen1 (hrs)
5	3	15	16	15	LF	\$56,937	\$103,914	0.302	0.84	1,955	633
	3	15	16	15	LF	\$47,937	\$112,506	0.327	0.71	3,118	1,005
20		15	32	15	LF	\$83,367	\$134,609	0.391	0.85	1,712	552
25	3		32	20	CC	\$104,770	\$137,494	0.399	1		
35			64	20	CC	\$136,600	\$188,945	0.549	1		
		15	32	10	CC	\$43,367	\$200,388	0.582	0	9,191	2,372
10	3	20		10	LF	\$48,552	\$236,693	0.687	0.5	12,717	3,091
	3	20			LF	\$22,552	\$313,403	0.91	0.28	19,975	4,858
15		20		10	LF	\$42,582	\$344,461	1	0.27	20,818	5,052
		20			LF	\$7,582	\$527,969	1.533	0	36,043	8,759

Table 6.4: System report for the 84 % renewable resource contribution

System architecture		Sensitivity case		Annual Electric Production(kwh/yr)			Annual Electric consumption (kWh/yr)			Emissions	
PV Array	5 kW			PV array	8,570	21%	AC primary load	25,404	94%	Pollutant	Emissions (kg/yr)
Wind turbine	3 HY-5KW	Solar Data Average(kWh/m ² /d):	5.82	Wind turbines	26,409	63%	Deferrable load	1,530	6%	Carbon dioxide	5,148
Gen 1	15 kW	Wind Data Average(m/s):	2.6	Gen 1	6,665	16%	Total	26,934	100%	Carbon monoxide	12.7
Battery	16 Surrette 6CS25P	Diesel Price(\$/L):	0.9	Total	41,644	100%	Cost summary		Unburned hydrocarbons	1.41	
Inverter	15 kW	PV Capital Cost Multiplier:	0.6	Excess electricity	10,258	kWh/yr	Total net present cost	\$103,914	Particulate matter	0.958	
Rectifier	15 kW	PV Replacement Cost Multiplier:	0.6	Unmet load	~0	kWh/yr	Levelized cost of energy	\$ 0.302/kWh	Sulfur dioxide	10.3	
Dispatch strategy	Load Following			Capacity shortage	2.25	kWh/yr	Operating cost	\$ 3,675/yr	Nitrogen oxides	113	

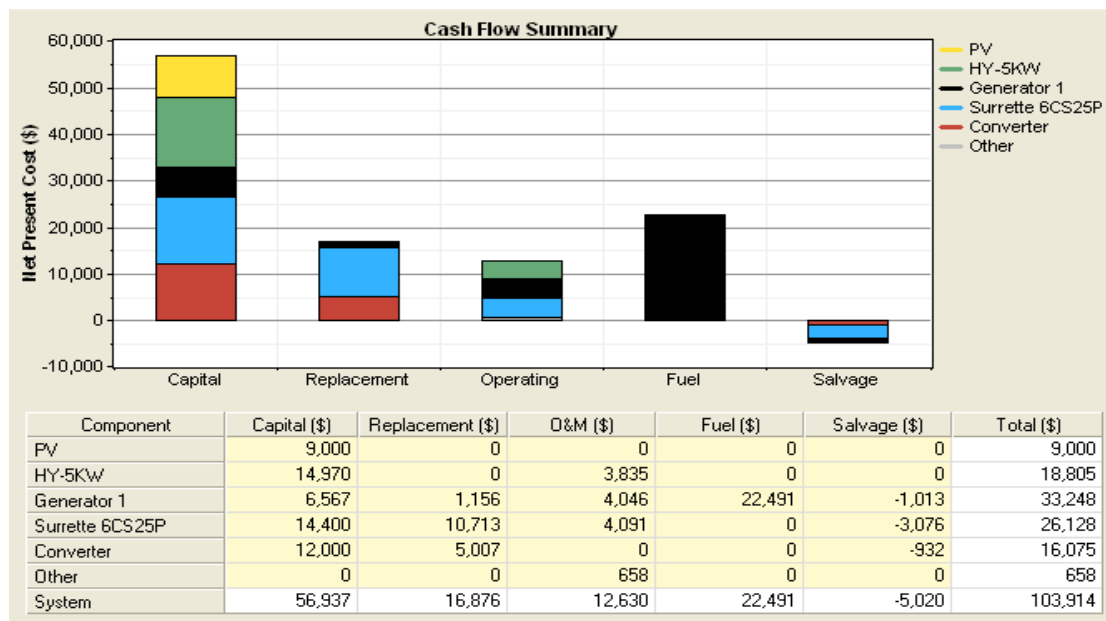


Figure 6.7: Cost summary for the 84 % renewable resource contribution

Table 6.5: System report for the 83 % renewable resource contribution

System architecture		Sensitivity case		Annual Electric Production (kWh/yr)			Annual Electric Consumption (kWh/yr)			Emissions	
PV Array	5 kW			PV array	8,570	21%	AC primary load	25,404	94%	Pollutant	Emissions (kg/yr)
Wind turbine	3 HY-5KW	Solar Data Average(kWh/m ² /d):	5.82	Wind turbines	26,409	62%	Deferrable load	1,530	6%	Carbon dioxide	5,721
Gen1	20 kW	Wind Data Average(m/s):	2.6	Gen 1	7,406	17%	Total	26,934	100%	Carbon monoxide	14.1
Battery	16 Surrette 6CS25P	Diesel Price(\$/L):	0.9	Total	42,385	100%	Cost summary		Unburned hydrocarbons	1.56	
Inverter	15 kW	PV Capital Cost Multiplier:	0.6	Excess electricity	10,774	kWh/yr	Total net present cost	\$106,553	Particulate matter	1.06	
Rectifier	15 kW	PV Replacement Cost Multiplier:	0.6	Unmet load	0	kWh/yr	Levelized cost of energy	\$ 0.309/kWh	Sulfur dioxide	11.5	
Dispatch strategy	Load Following			Capacity shortage	0	kWh/yr	Operating cost	\$ 3,802/yr	Nitrogen oxides	126	

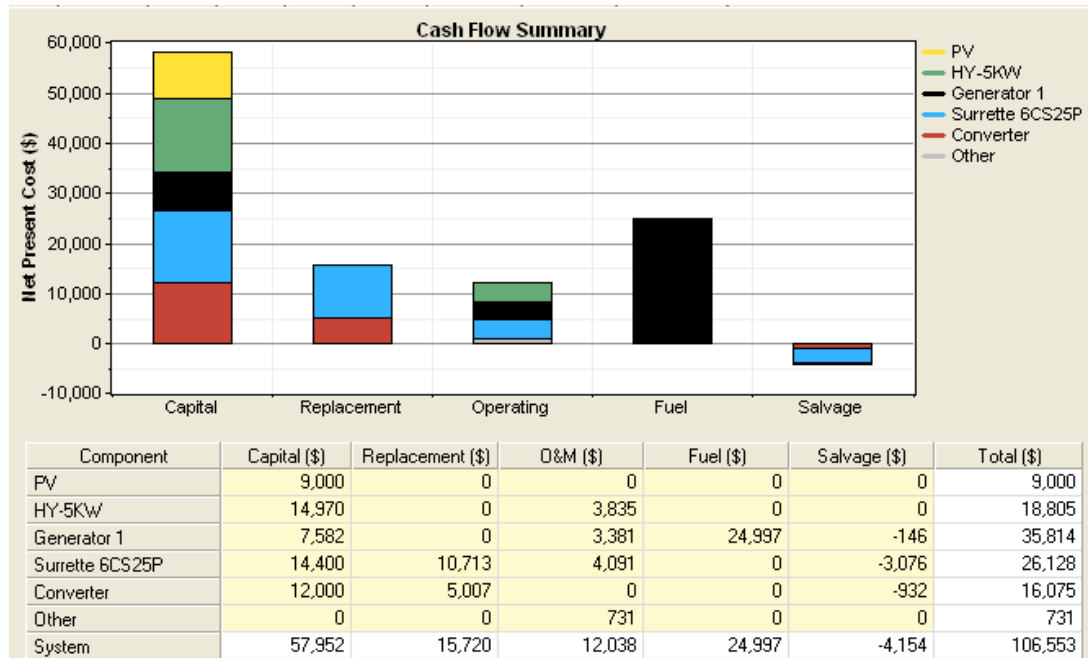


Figure 6.8: Cost summary for the 83 % renewable resource contribution

Table 6.6: System report for the 96% renewable resource contribution

System architecture		Sensitivity case		Annual Electric Production (kWh/yr)			Annual Electric Consumption (kWh/yr)			Emissions	
PV Array	10 kW			PV array	17,139	38%	AC primary load	25,404	94%	Pollutant	Emissions (kg/yr)
Wind turbine	3 HY-5KW	Solar Data Average(kWh/m ² /d):	5.82	Wind turbines	26,409	58%	Deferrable load	1,529	6%	Carbon dioxide	1,396
Gen 1	15 kW	Wind Data Average(m/s):	2.6	Gen 1	1,807	4%	Total	26,933	100%	Carbon monoxide	3.45
Battery	32 Surrette 6CS25P	Diesel Price(\$/L):	0.9	Total	45,356	100%	Cost summary		Unburned hydrocarbons	0.382	
Inverter	15 kW	PV Capital Cost Multiplier:	0.6	Excess electricity	12,288	kWh/yr	Total net present cost	\$118,315	Particulate matter	0.26	
Rectifier	15 kW	PV Replacement Cost Multiplier:	0.6	Unmet load	0	kWh/yr	Levelized cost of energy	\$ 0.344/kWh	Sulfur dioxide	2.8	
Dispatch strategy	Load Following			Capacity shortage	0	kWh/yr	Operating cost	\$ 2,971/y	Nitrogen oxides	30.7	

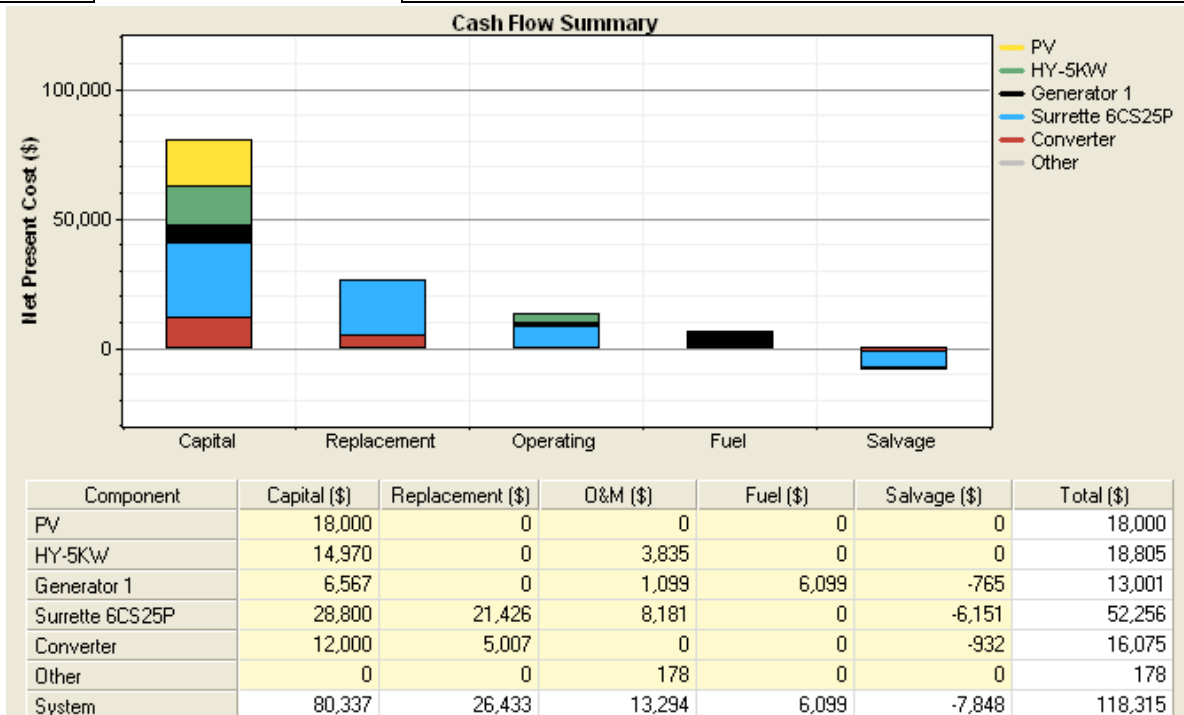


Figure 6.9: Cost summary for the 96 % renewable resource contribution

Table 6.7: System report for the 100% renewable resource contribution

System architecture		Sensitivity case		Annual Electric Production (kWh/yr)			Annual Electric Consumption (kWh/yr)			Emissions	
PV Array	20 kW			PV array	34,279	56%	AC primary load	25,397	94%	Pollutant	Emissions (kg/yr)
Wind turbine	3 HY-5KW	Solar Data Average(kWh/m²/d):	5.82	Wind turbines	26,409	43%	Deferrable load	1,529	6%	Carbon dioxide	46.4
Gen 1	6 kW	Wind Data Average(m/s):	2.6	Gen 1	61	0%	Total	26,926	100%	Carbon monoxide	0.115
Battery	32 Surrette 6CS25P	Diesel Price(\$/L):	0.9	Total	60,748	100%	Cost summary		Unburned hydrocarbons	0.0127	
Inverter	20 kW	PV Capital Cost Multiplier:	0.6	Excess electricity	27,341	kWh/yr	Total net present cost	\$129,593	Particulate matter	0.0086	
Rectifier	20 kW	PV Replacement Cost Multiplier:	0.6	Unmet load	6.8	kWh/yr	Levelized cost of energy	\$ 0.376/kWh	Sulfur dioxide	0.0932	
Dispatch strategy	Load Following			Capacity shortage	15	kWh/yr	Operating cost	\$ 2,571/y	Nitrogen oxides	1.02	

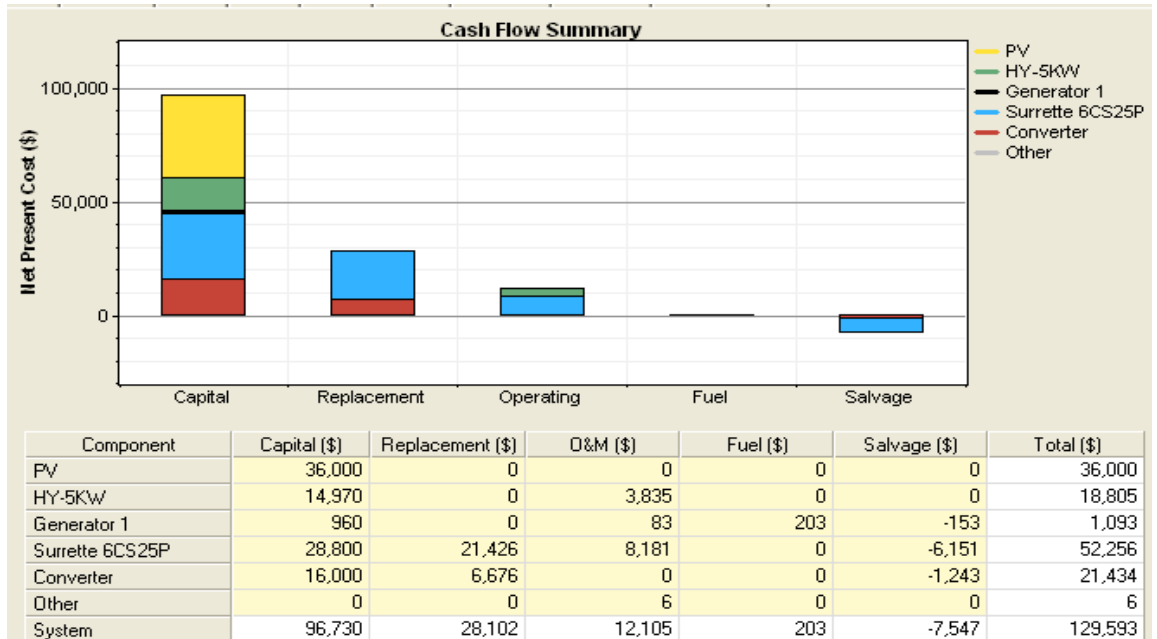


Figure 6.10: Cost summary for the 100% renewable resource contribution

Sensitivity analysis was also carried out and figure 6.11 shows the variation of PV capital cost multiplier against diesel price for a fixed average wind speed of 2.6 m/s (measured at 2 meters) and average solar radiation of 5.82 kWh/m²/day. In the figure, the net present cost of the most cost-effective set-up for a particular set of diesel and PV prices is also included.

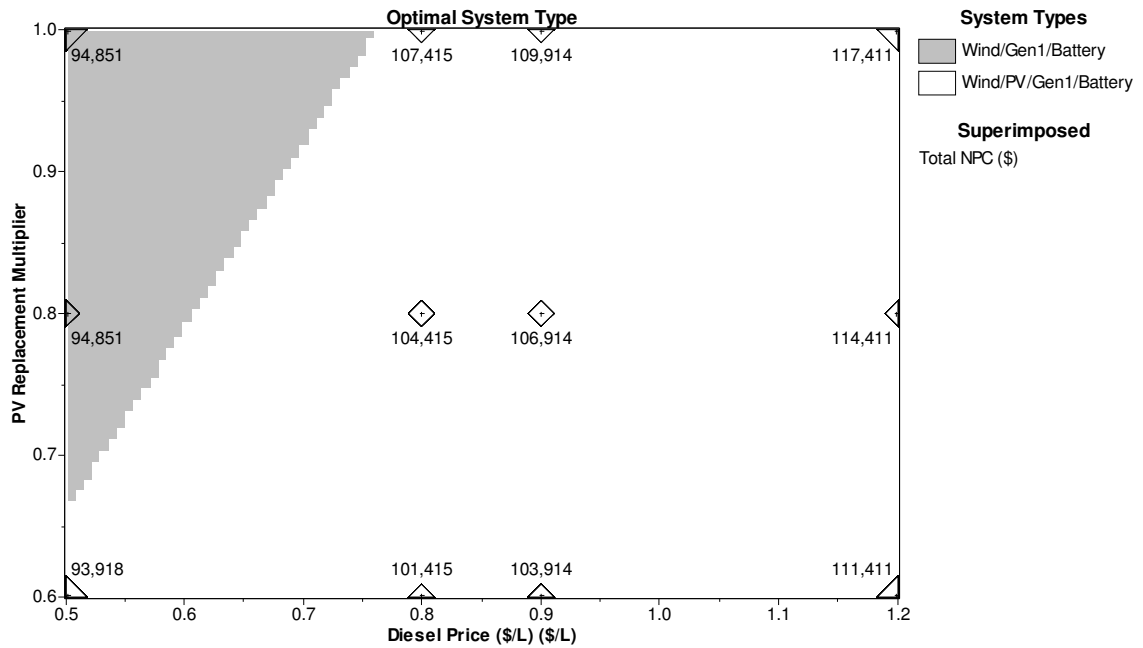


Figure 6.11: Sensitivity of PV cost to diesel price with some important NPCs labeled

In this figure it can be seen that the wind plays big role in supplying energy to the community. At this point, it must be known that this is not due to more availability of wind potential than solar energy potential; rather it is because of wind turbine used. The wind turbine used in the design of the system is one with small cut-in wind speed, 2m/s, and also have small capital cost when compared to majority of turbines in the market.

From figure 6.11, it is observed that for a diesel price of less than \$0.8/l with PV cost multiplier greater than 0.7 Wind/Generator/Battery/Converter systems is favourable while for diesel price higher than \$0.8/l Wind/PV/Generator/Battery/Converter system is favourable for all PV capital cost multipliers.

6.2. Conclusion

A hybrid power generation system which comprises of PV arrays, wind turbines and diesel generator with battery banks and power conditioning units has been discussed in this thesis to achieve a cost effective system configuration which is supposed to supply electricity to model community of 100 households which equipped with a health clinic and school to improve the life of people in the rural areas where electricity from the main grid has not reached yet. Before the design of the hybrid system was started, the wind energy and solar energy potentials of the area under study had been studied. Then, based on these potentials, a design of a standalone electric power supply system for a model community has been conducted.

The study of the renewable potentials of the site is based on the recently recorded data (2003-2005) obtained from the NMA. The data regarding wind speed were recorded over 24 hours using data logger attached to cup anemometer at a height of 2 meters for 3 successive years. Regarding solar energy potential there is no accurately recorded solar radiation database in the country, instead only sunshine hour data was available. Therefore, empirical formulas which are able to incorporate the available sunshine hour data and provide the required solar radiation data were used to determine the potential of the site. The results obtained from empirical formulas were also cross-checked against satellite data obtained from other sources such as NASA and SWERA [NASA, 2010], [SWERA, 2011]. The analysis of the renewable energy resources data has been carried out by HOMER software. From the results, the wind energy potential of the site is found to be considerable, although it may not be sufficient for a large independent wind farm; it is viable option if incorporated into other energy conversion systems such as PV, diesel generator and battery. The results also confirmed the availability of huge utilizable solar energy at the site.

The results obtained from the software give numerous alternatives of feasible hybrid systems with different levels of renewable resources penetration which their choice is restricted by changing the net present cost of each set up. The COE of the feasible setups in this study, which is in the range of 30 to 40 cents per kilo watt hour, are high compared to the current

global electricity tariff and the tariff in the country (<5 cents/kWh). However, considering the shortage of electricity in the country (<20% coverage) and absence of electricity usage in rural areas (<2% coverage), this cost should not be taken as a decisive factor. Instead other issues such as the role of a standalone hybrid system in protecting the environment from degradation, the improvement of life of people living in rural area, development of clean energy, the future situation regarding fossil fuel sources, and its contribution to the reduction of pollutant emissions into the environment should be taken in to account. Taking these issues into account the free solar and wind energy of the country should be utilized to improve the quality of life of the communities living in rural areas.

6.3. Recommendations

The following recommendations are made out of this research; some of them are directed to the researchers while the others are directed to decision makers.

- Ethiopia has a huge potential of renewable energy resources which can be used for rural electrification through the off-grid system. There are, however, many challenges like low purchasing power of the rural community, unfavorable conditions towards the utilization of renewable energies, absence of awareness how to use these resources, etc. Thus, the author of this work recommends that the government, non-governmental organizations and the private sectors should make combined efforts to overcome these challenges by using more flexible approaches to improve the current poor status of rural electrification in Ethiopia.
- The implementation for this hybrid system as a pilot system in country can be done if a subsidy is available for this project, this will make it possible for more research, study and analysis.
- As far as the environmental aspects are concerned, this kind of hybrid systems have to be wide spread in order to cover the energy demands of rural communities, and in that way to help reduce the green house gases and the pollution of the environment.
- Similar solar and wind energy potentials assessment can be conducted for other sites in the country.

7. References

- Ali, B. et al, (2010) “Hybrid Photovoltaic Diesel System in a Cable Car Resort Facility”. European Journal of Scientific Research, Vol.26 No.1.
- Barley, C.D. and Winn, C.B., (1996) “Optimal dispatch strategy in remote hybrid power systems”. Solar Energy, Vol. 58, pp 165-179
- Bimrew, T., (2007) *Comparative Analysis of Feasibility of Solar PV, Wind and Micro Hydropower Generation for Rural Electrification in the Selected Sites of Ethiopia*. MSc. Thesis, Addis Ababa University
- Blue Bonnet Solar, (Jan., 2011): www.bluebonnetsolar.com
- Breeze, P. et al. (2009) *Renewable Energy Focus Handbook*. Oxford, UK: Elsevier Inc.
- Celik, A.N. (2002), “Optimization and techno-economic analysis of autonomous photovoltaic-wind-hybrid energy systems in comparison to single photovoltaic and wind systems.” Energy Conversion and Management, Vol. 43, No. 18.
- CIA the world fact book, 2010,
<http://www.umsl.edu/services/govdocs/wofact2007/geos/et.html#People>
- Danish Wind Industry Association, (Jan., 2011), <http://www.windpower.org/en/tour>
- Drake, F. and Mulugetta, Y., (1996), “Assessment of solar and wind energy resources in Ethiopia: Part 2. Wind energy”. Solar Energy, Vol. 51, pp 205-217.
- Duffie, J.A. and Beckman, W.A., (2006) *Solar Engineering of Thermal Processes*. 3rd ed. New Jersey: John Wiley and Sons, Inc.
- EcoBusinessLinks, (March, 2011), <http://www.ecobusinesslinks.com>

- Fernando D. B., Hernán D. B., and Ricardo J. M., (2007) *Wind Turbine Control Systems: Principles, Modelling and Gain Scheduling Design*. London: Springer-Verlag.
- Getachew, B., (2009) *Study into the Potential and Feasibility of a Standalone Solar-wind Hybrid Electric Energy Supply System: For Application in Ethiopia*. Ph.D Dissertation, Royal Institute of Technology, KTH.
- Gipe, P., (2004) *Wind Power: Renewable Energy for Home, Farm, and Business*. Chelsea Green Publishing Company.
- Gupta, A., et al., (2008) “Computerized Modeling of Hybrid Energy System-Part I: Problem Formulation and Model Development.” 5th ICECE, Dhaka, Bangladesh.
- HOMER, the micropower optimization model, ver. 2.67 Beta (April, 2008), <http://www.nrel.gov/homer>
- Hulk Energy Machinery, (Jan., 2011), <http://www.hulkenergy.com>
- Kanase-Patil A.B., Saini R.P., Sharma M.P., 2010 “Integrated Renewable Energy Systems for Off Grid Rural Electrification of Remote Area”, *Renewable Energy*, Vol. 35, pp. 1342–1349
- Leake, E.W. (2010) *Genset-Solar-Wind Hybrid Power System of Off-Grid Power Station for Rural Applications: Sustainable off-grid power station for rural applications*. MSc Thesis, Technical University of Delft.
- Luque, A. and Hegedus, S., (Ed) (2003) *Handbook of Photovoltaic Science and Engineering*. West Sussex, England: John Wiley & Sons Ltd.
- Mathew, S., (2006) *Wind Energy: Fundamentals, Resource Analysis and Economics*. Berlin Heidelberg: Springer-Verlag.

- Mulugeta Y., (1999) “Energy in Rural Ethiopia: Consumption Patterns, Associated Problems, and Prospects for a Sustainable Energy Strategy”, Energy Sources, Part A: Recovery, Utilization, and Environmental Effects,
- NASA Science News, (Jan., 2011), <http://science.nasa.gov/science-news>
- Nfah, E., Ngundam, J., and Tchinda, R. (2007) “Modelling of solar/diesel/battery hybrid power systems for far-north Cameroon”. Renewable Energy, Vol.32, p 832–844
- Nfah, E.M. et al. (2008). “Simulation of off-grid generation options for remote villages in Cameroon”. Renewable Energy, Vol. 33, p 1064–1072
- Nfah, E.M. and Ngundam, J.M. (2009). “Feasibility of pico-hydro and photovoltaic hybrid power systems for remote villages in Cameroon”. Renewable Energy, Vol. 34, p 1445–1450.
- Nfah, E., Ngundam, J., and Kenne, G. (2010) “Economic evaluation of small-scale photovoltaic hybrid systems for mini-grid applications in far north Cameroon”. Renewable Energy, Vol.35, p 2391-2398.
- Patel, M.R., (2006) *Wind and Solar Power Systems: Design, Analysis, and Operation*. 2nd Ed. Boca Raton: Taylor & Francis Group.
- Rivera, M.R., (2008) *Small Wind / Photovoltaic Hybrid Renewable Energy System Optimization*. MSc. Thesis, University of Puerto Rico.
- Ramos, C., (2005) *Determination of favorable conditions for the development of a wind power farm in Puerto Rico*. MSc. Thesis, University of Puerto Rico.
- Renewable Energy World, (Nov., 2010), <http://renewableenergyworld.com>
- Solarbuzz, (March, 2011), <http://www.solarbuzz.com/industry-news>

Solar Panel Price, (Jan, 2010), <http://solarpanelprices.org>

SWERA-Data for Solar and Wind Renewable Energy, (Jan., 2011): <http://swera.unep.net/>

Tzanakis, I., (2006) “*Combining Wind and Solar Energy to Meet Demands in the Built Environment*”: (*Glasgow-Heraklion Crete Analysis*). MSc Thesis, University of Strathclyde.

Wagner, H. and Mathur, J., (2009) *Introduction to Wind Energy Systems: Basics, Technology and Operation*. Berlin Heidelberg: Springer-Verlag.

Wang, C., (2006) *Modeling and Control of Hybrid Wind/Photovoltaic/Fuel Cell Distributed Generation Systems*. Ph.D Dissertation, Montana State University.

Wind Turbines, (Jan., 2011), <http://www.windturbines.net/wiki>

Wolde-Ghiorgis, W., (1988) “Wind energy survey in Ethiopia”. *Solar Wind Technology*; Vol. 5, pp 341-351.

8. Appendix A: Overall Optimization Results Table

Table 8.1: Overall optimization results

PV (kW)	HY-5	Gen1 (kW)	Battery	Converter (kW)	Dispatch strategy	Initial capital	Total NPC	COE (\$/kWh)	Renewable fraction	Diesel (L)	Gen1 (hrs)
5	3	15	16	15	LF	\$56,937	\$103,914	0.302	0.84	1,955	633
5	3	20	16	15	LF	\$57,952	\$106,553	0.309	0.83	2,173	529
10	3	15	16	15	LF	\$65,937	\$108,489	0.315	0.89	1,655	537
5	2	15	16	15	LF	\$51,947	\$109,014	0.317	0.74	2,703	874
5	3	15	16	20	LF	\$60,937	\$109,213	0.317	0.84	1,951	632
10	2	15	16	15	LF	\$60,947	\$109,325	0.318	0.83	2,129	691
10	3	20	16	15	LF	\$66,952	\$111,272	0.323	0.87	1,865	454
5	3	20	16	20	LF	\$61,952	\$111,569	0.324	0.83	2,148	523
5	2	20	16	15	LF	\$52,962	\$111,649	0.324	0.72	2,965	722
10	2	20	16	15	LF	\$61,962	\$112,311	0.326	0.81	2,390	582
	3	15	16	15	LF	\$47,937	\$112,506	0.327	0.71	3,118	1,005
	3	15	16	10	LF	\$43,937	\$112,660	0.327	0.69	3,483	1,128
10	3	15	16	20	LF	\$69,937	\$113,580	0.33	0.89	1,636	531
5	2	15	16	20	LF	\$55,947	\$114,437	0.332	0.74	2,708	875
10	2	15	16	20	LF	\$64,947	\$114,514	0.333	0.83	2,118	687
5	2	15	16	10	LF	\$47,947	\$114,926	0.334	0.69	3,450	1,120
5	3	15	16	10	LF	\$52,937	\$115,045	0.334	0.77	3,040	987
	3	20	16	15	LF	\$48,952	\$115,055	0.334	0.7	3,388	825
15	2	15	16	15	LF	\$69,947	\$115,728	0.336	0.87	1,959	636
10	1	15	16	15	LF	\$55,957	\$116,088	0.337	0.72	2,990	968
10	3	20	16	20	LF	\$70,952	\$116,116	0.337	0.87	1,828	445
15	3	15	16	15	LF	\$74,937	\$116,144	0.337	0.91	1,562	507
5	2	20	16	20	LF	\$56,962	\$116,589	0.339	0.72	2,937	715
10	2	15	32	15	LF	\$75,347	\$116,780	0.339	0.92	857	278
5	3	15	32	15	LF	\$71,337	\$117,050	0.34	0.91	1,064	345
10	2	20	16	20	LF	\$65,962	\$117,384	0.341	0.81	2,370	577
	3	15	16	20	LF	\$51,937	\$117,794	0.342	0.71	3,114	1,003
10	1	20	16	15	LF	\$56,972	\$117,960	0.343	0.7	3,212	782
10	3	15	32	15	LF	\$80,337	\$118,315	0.344	0.96	530	172
10	2	20	32	15	LF	\$76,362	\$118,571	0.344	0.91	961	234
5	3	20	32	15	LF	\$72,352	\$118,808	0.345	0.9	1,175	286
15	3	20	16	15	LF	\$75,952	\$119,073	0.346	0.9	1,778	433
15	2	20	16	15	LF	\$70,962	\$119,084	0.346	0.85	2,230	543
15	1	15	16	15	LF	\$64,957	\$119,800	0.348	0.79	2,639	856
10	2	15	32	20	LF	\$79,347	\$120,081	0.349	0.93	715	231
10	3	20	32	15	LF	\$81,352	\$120,273	0.349	0.95	633	154
	3	20	16	20	LF	\$52,952	\$120,354	0.35	0.7	3,384	824
10	3	15	32	20	LF	\$84,337	\$120,366	0.35	0.98	302	98

15	2	15	16	20	LF	\$73,947	\$120,948	0.351	0.87	1,950	633
15	1	15	32	15	LF	\$79,357	\$121,003	0.351	0.91	960	311
10	2	20	32	20	LF	\$80,362	\$121,133	0.352	0.93	760	185
15	3	15	16	20	LF	\$78,937	\$121,145	0.352	0.91	1,537	499
10	1	15	16	20	LF	\$59,957	\$121,209	0.352	0.72	2,975	962
10	3	20	32	20	LF	\$85,352	\$121,235	0.352	0.98	316	77
5	3	15	32	20	LF	\$75,337	\$121,239	0.352	0.91	984	318
	3	20	16	10	LF	\$44,952	\$121,302	0.352	0.65	4,193	1,021
15	2	15	32	15	LF	\$84,347	\$121,312	0.352	0.96	548	178
5	3	20	32	20	LF	\$76,352	\$122,397	0.355	0.91	1,047	255
15	2	15	32	20	LF	\$88,347	\$122,651	0.356	0.98	271	88
10	1	15	16	10	LF	\$51,957	\$122,666	0.356	0.67	3,783	1,228
15	1	20	16	15	LF	\$65,972	\$122,723	0.356	0.78	2,920	711
15	1	20	32	15	LF	\$80,372	\$122,902	0.357	0.9	1,076	262
15	3	10	32	15	LF	\$88,322	\$123,134	0.358	0.98	277	135
10	2	15	16	10	LF	\$56,947	\$123,142	0.358	0.75	3,398	1,103
5	3	15	16	10	CC	\$52,937	\$123,314	0.358	0.74	3,658	1,085
10	1	20	16	20	LF	\$60,972	\$123,497	0.359	0.7	3,224	785
20	2	15	16	15	LF	\$78,947	\$123,598	0.359	0.89	1,885	612
15	2	20	32	20	LF	\$89,362	\$123,681	0.359	0.98	296	72
15	2	20	32	15	LF	\$85,362	\$123,747	0.359	0.95	686	167
5	1	20	16	15	LF	\$47,972	\$123,949	0.36	0.55	4,251	1,035
10	3	15	16	10	LF	\$61,937	\$123,952	0.36	0.81	3,034	985
15	3	20	16	20	LF	\$79,952	\$123,974	0.36	0.9	1,746	425
15	2	20	16	20	LF	\$74,962	\$124,307	0.361	0.85	2,210	538
10	3	10	32	20	CC	\$83,322	\$124,692	0.362	0.95	635	257
5	2	15	4	10	LF	\$37,147	\$124,756	0.362	0.59	5,396	1,742
15	3	6	32	20	CC	\$87,730	\$124,778	0.362	0.98	276	182
20	3	15	16	15	LF	\$83,937	\$124,786	0.362	0.92	1,537	499
15	1	15	32	20	LF	\$83,357	\$124,805	0.363	0.92	853	276
15	1	15	16	20	LF	\$68,957	\$125,081	0.363	0.79	2,634	854
5	2	15	32	15	LF	\$66,347	\$125,284	0.364	0.79	2,055	663
15	3	15	32	15	LF	\$89,337	\$125,302	0.364	0.98	391	127
15	3	10	32	20	LF	\$92,322	\$125,456	0.364	0.99	84	40
	3	15	4	10	LF	\$33,137	\$125,692	0.365	0.58	5,642	1,817
10	3	10	32	15	CC	\$79,322	\$125,845	0.366	0.92	1,060	445
10	3	15	32	15	CC	\$80,337	\$125,855	0.366	0.92	1,069	314
15	1	20	32	20	LF	\$84,372	\$125,863	0.366	0.92	904	220
20	1	15	32	15	LF	\$88,357	\$126,014	0.366	0.95	684	222
	3	15	16	10	CC	\$43,937	\$126,171	0.366	0.63	4,476	1,299
15	3	15	32	20	LF	\$93,337	\$126,285	0.367	0.99	89	29
5	2	20	32	15	LF	\$67,362	\$126,413	0.367	0.78	2,173	529
20	3	6	32	15	LF	\$92,730	\$126,553	0.368	0.99	152	123
20	1	15	16	15	LF	\$73,957	\$126,599	0.368	0.84	2,493	809
5	2	15	16	10	CC	\$47,947	\$126,613	0.368	0.64	4,306	1,273
10	3	20	32	15	CC	\$81,352	\$126,758	0.368	0.92	1,122	236
20	2	10	32	15	LF	\$92,332	\$126,773	0.368	0.98	335	163

	2	20	16	10	LF	\$39,962	\$126,829	0.368	0.51	5,015	1,221
10	3	15	32	20	CC	\$84,337	\$126,947	0.369	0.94	762	236
10	1	15	32	15	LF	\$70,357	\$127,149	0.369	0.79	1,998	645
15	3	20	32	20	LF	\$94,352	\$127,266	0.37	0.99	103	25
5	3	15	4	10	LF	\$42,137	\$127,294	0.37	0.67	5,146	1,665
20	2	20	16	15	LF	\$79,962	\$127,380	0.37	0.87	2,177	530
15	3	20	32	15	LF	\$90,352	\$127,560	0.37	0.97	509	124
20	1	15	32	20	LF	\$92,357	\$127,713	0.371	0.97	432	140
10	1	20	32	15	LF	\$71,372	\$127,774	0.371	0.79	2,074	505
20	3	20	16	15	LF	\$84,952	\$127,787	0.371	0.91	1,758	428
15	1	20	16	20	LF	\$69,972	\$127,905	0.371	0.78	2,900	706
5	3	20	16	10	LF	\$53,952	\$128,177	0.372	0.72	4,046	985
	3	15	32	15	LF	\$62,337	\$128,533	0.373	0.76	2,449	789
20	1	20	32	15	LF	\$89,372	\$128,533	0.373	0.94	834	203
20	2	10	32	20	LF	\$96,332	\$128,572	0.373	0.99	109	52
20	1	20	32	20	LF	\$93,372	\$128,640	0.374	0.97	456	111
20	2	15	16	20	LF	\$82,947	\$128,663	0.374	0.89	1,864	605
5	2	20	16	10	LF	\$48,962	\$128,745	0.374	0.63	4,522	1,101
15	3	10	32	20	CC	\$92,322	\$129,102	0.375	0.98	328	137
10	3	20	32	20	CC	\$85,352	\$129,209	0.375	0.93	896	208
10	2	15	32	15	CC	\$75,347	\$129,236	0.375	0.85	1,744	516
20	2	6	32	20	CC	\$91,740	\$129,279	0.376	0.97	385	255
15	2	10	32	20	CC	\$87,332	\$129,328	0.376	0.94	757	316
20	2	15	32	15	LF	\$93,347	\$129,329	0.376	0.97	481	156
5	1	20	16	20	LF	\$51,972	\$129,449	0.376	0.54	4,261	1,037
15	3	6	32	15	CC	\$83,730	\$129,455	0.376	0.94	897	585
20	2	15	32	20	LF	\$97,347	\$129,463	0.376	0.99	120	39
5	3	10	32	15	CC	\$70,322	\$129,576	0.376	0.84	1,881	779
20	3	6	32	20	LF	\$96,730	\$129,593	0.376	1	18	13
20	3	15	16	20	LF	\$87,937	\$129,743	0.377	0.92	1,509	490
	3	20	32	15	LF	\$63,352	\$129,778	0.377	0.75	2,604	634
20	1	20	16	15	LF	\$74,972	\$129,927	0.377	0.82	2,776	676
5	2	15	32	20	LF	\$70,347	\$129,985	0.378	0.79	2,013	648
5	1	20	16	10	LF	\$43,972	\$130,035	0.378	0.5	5,048	1,229
10	2	20	32	15	CC	\$76,362	\$130,080	0.378	0.85	1,822	389
5	2	15	4	15	LF	\$41,147	\$130,114	0.378	0.59	5,396	1,742
15	3	15	32	20	CC	\$93,337	\$130,192	0.378	0.98	361	113
15	2	15	32	20	CC	\$88,347	\$130,526	0.379	0.94	819	257
10	2	10	32	15	CC	\$74,332	\$130,544	0.379	0.85	1,771	732
20	2	20	32	20	LF	\$98,362	\$130,569	0.379	0.99	144	35
10	3	15	16	10	CC	\$61,937	\$130,837	0.38	0.78	3,554	1,059
25	3	10	16	15	LF	\$91,922	\$130,845	0.38	0.94	1,273	616
	3	15	4	15	LF	\$37,137	\$131,050	0.381	0.58	5,642	1,817
5	3	15	32	15	CC	\$71,337	\$131,074	0.381	0.83	2,057	616
5	2	20	32	20	LF	\$71,362	\$131,143	0.381	0.78	2,128	518
15	1	15	16	10	LF	\$60,957	\$131,288	0.381	0.73	3,758	1,220
5	3	20	32	15	CC	\$72,352	\$131,424	0.382	0.83	2,117	458

20	3	6	32	20	CC	\$96,730	\$131,495	0.382	0.99	136	89
15	2	15	32	15	CC	\$84,347	\$131,666	0.382	0.91	1,284	379
20	1	15	16	20	LF	\$77,957	\$131,693	0.382	0.84	2,476	803
20	3	10	32	15	LF	\$97,322	\$131,713	0.383	0.99	251	122
15	3	15	32	15	CC	\$89,337	\$131,760	0.383	0.95	849	253
20	2	20	32	15	LF	\$94,362	\$131,947	0.383	0.96	628	153
25	2	15	16	15	LF	\$87,947	\$132,028	0.383	0.91	1,848	600
15	3	20	32	15	CC	\$90,352	\$132,038	0.383	0.95	849	178
15	2	15	16	10	LF	\$65,947	\$132,049	0.384	0.79	3,391	1,101
15	3	20	32	20	CC	\$94,352	\$132,097	0.384	0.97	453	106
15	3	10	32	15	CC	\$88,322	\$132,188	0.384	0.94	885	371
10	2	15	16	10	CC	\$56,947	\$132,233	0.384	0.71	4,075	1,213
10	2	10	32	20	CC	\$78,332	\$132,234	0.384	0.87	1,535	644
5	3	20	16	10	CC	\$53,952	\$132,338	0.384	0.7	4,357	1,031
15	2	10	32	15	CC	\$83,332	\$132,369	0.384	0.9	1,312	546
	3	20	16	10	CC	\$44,952	\$132,375	0.384	0.61	5,001	1,169
20	3	20	16	20	LF	\$88,952	\$132,575	0.385	0.91	1,717	418
20	2	20	16	20	LF	\$83,962	\$132,594	0.385	0.88	2,140	521
15	2	20	32	15	CC	\$85,362	\$132,601	0.385	0.9	1,347	288
10	1	15	32	20	LF	\$74,357	\$132,631	0.385	0.79	2,007	647
5	3	15	4	15	LF	\$46,137	\$132,652	0.385	0.67	5,146	1,665
15	3	15	16	10	LF	\$70,937	\$132,952	0.386	0.83	3,034	985
10	2	15	4	10	LF	\$46,147	\$133,054	0.386	0.66	5,349	1,728
	3	15	32	20	LF	\$66,337	\$133,287	0.387	0.76	2,410	775
	2	20	16	20	LF	\$47,962	\$133,293	0.387	0.52	4,720	1,149
15	2	20	32	20	CC	\$89,362	\$133,363	0.387	0.93	999	232
25	3	15	16	15	LF	\$92,937	\$133,429	0.388	0.93	1,512	491
5	1	15	16	10	CC	\$42,957	\$133,438	0.388	0.49	5,195	1,518
10	1	20	32	20	LF	\$75,372	\$133,475	0.388	0.78	2,099	511
20	3	10	32	20	LF	\$101,322	\$133,495	0.388	1	23	11
25	1	15	32	15	LF	\$97,357	\$133,580	0.388	0.96	585	190
5	3	10	32	20	CC	\$74,322	\$133,701	0.388	0.85	1,804	747
20	3	15	32	15	LF	\$98,337	\$134,079	0.389	0.98	376	122
20	2	10	32	20	CC	\$96,332	\$134,117	0.39	0.97	480	198
25	1	15	32	20	LF	\$101,357	\$134,117	0.39	0.98	253	82
5	3	10	32	10	CC	\$66,322	\$134,345	0.39	0.8	2,467	1,118
25	1	15	16	15	LF	\$82,957	\$134,398	0.39	0.86	2,410	782
20	3	15	32	20	LF	\$102,337	\$134,436	0.39	1	31	10
20		15	32	15	LF	\$83,367	\$134,609	0.391	0.85	1,712	552
	3	15	32	10	LF	\$58,337	\$134,643	0.391	0.71	3,207	1,038
5	2	20	16	10	CC	\$48,962	\$134,722	0.391	0.61	4,967	1,171
15		20	16	15	LF	\$60,982	\$134,975	0.392	0.64	4,202	1,023
5	2	15	4	10	CC	\$37,147	\$135,034	0.392	0.56	6,098	1,931
5	3	15	4	10	CC	\$42,137	\$135,059	0.392	0.64	5,679	1,810